10.4 FACTORS CONTROLLING COMPARATIVE INHALED DOSE

As discussed in Section 10.1, comprehensive characterization of the exposure-dose-response continuum is the fundamental objective of any dose-response assessment. Within human and interspecies differences in anatomical and physiological characteristics, the physicochemical properties of the inhaled aerosol, the diversity of cell types that may be affected, and a myriad of mechanistic and metabolic differences all combine to make the characterization particularly complex for the respiratory tract as the portal of entry. This section attempts to discuss these factors within the exposure-dose-response context in order to present unifying concepts. These concepts are used to construct a framework by which to

TABLE 10-3. MORPHOLOGY, CYTOLOGY, HISTOLOGY, FUNCTION, AND STRUCTURE OF THE RESPIRATORY TRACT AND REGIONS USED IN THE ICRP66 (1994) HUMAN DOSIMETRY MODEL

Functions	Cytology (Epithelium)	Histology (Walls)	Generation Number	Anatomy	Regions used in Model: New		Regions used in Model: Old[d]	Zones (Air)		Location		Airway Surface[a]	Number of Airways
Air Conditioning Temperature and Humidity, and Cleaning; Fast Particle Clearance; Air Conduction	Respiratory Epithelium with Goblet Cells Cell Types: • Ciliated Cells • Nonciliated Cells: Goblet Cells Mucous (Secretory) Cells Serous Cells Brush Cells Endocrine Cells Basal Cells Intermediate Cells	Mucous Membrane, Respiratory Epithelium (Pseudostratified, Ciliated, Mucous), Glands Mucous Membrane, Respiratory or Stratified Epithelium, Glands		Anterior Nasal Passages	ET_1		(N-P)	Conduction	0.175 x 10^{-3} m^3 (Anatomical Dead Space)	Extrathoracic	Extrapulmonary	2 x 10^{-3} m^2	———
				Nose / Mouth / Pharynx / Posterior / Larynx / Esophagus	ET_2	LN_{ET}						4.5 x 10^{-2} m^2	———
		Mucous Membrane, Respiratory Epithelium Cartilage Rings, Glands	0	Trachea	BB	$LN_{TH}^{(e)}$	(T-B)			Thoracic	Pulmonary	2.9 x 10^{-2} m^2 (a)	511 (a)
			1	Main Bronchi									
		Mucous Membrane, Respiratory Epithelium, Cartilage plates, Smooth Muscle Layer, Glands	2-8	Bronchi									
	Respiratory Epithelium with Clara Cells (No Goblet Cells) Cell Types: • Ciliated Cells • Nonciliated Cells: Clara (Secretory) Cells	Mucous Membrane, Respiratory Epithelium, No Cartilage, No Glands, Smooth Muscle Layer	9-14	Bronchioles	bb							2.4 x 10^{-1} m^2 (a)	6.5 x 10^4 (a)
		Mucous Membrane, Single-Layer Respiratory Epithelium, Less Ciliated, Smooth Muscle Layer	15	Terminal Bronchioles									
Air Conduction; Gas Exchange; Slow Particle Clearance	Respiratory Epithelium Consisting Mainly of Clara Cells(Secretory) and Few Ciliated Cells	Mucous Membrane, Single-Layer Respiratory Epithelium of Cuboidal Cells, Smooth Muscle Layer	16-18	Respiratory Bronchioles	AI		P	Gas-Exchange Transitory	0.2 x 10^{-3} m^3			7.5 m^2	4.6 x 10^5 (a)
Gas Exchange; Very Slow Particle Clearance	Squamous Alveolar Epithelial Cells (Type I), Covering 93% of Alveolar Surface Areas Cuboidal Alveolar Epithelial Cells (Type II, Surfactant-Producing), Covering 7% of Alveolar Surface Area Alveolar Macrophages	Wall Consists of Alveolar Entrance Rings, Squamous Epithelial Layer, Surfactant	(c)	Alveolar Ducts					4.5 x 10^{-3} m^3			140 m^2	4.5 x 10^7 (b)
		Interalveolar Septa Covered by Squamous Epithelium, Containing Capillaries, Surfactant	(c)	Alveolar Sacs									
				Lymphatics			L						

[a] Dimensions from three sources (James, 1988; adapted from Weibel, 1963; Yeh and Schum, 1980; and Phalen et al., 1985) were averaged after all were adjusted to a functional residual capacity (FRC) of 3.3 × 10^3 m^3 (Yu and Diu, 1982a; James, 1988).

[b] Calculated from Hansen and Ampaya (1975) and scaled to a functional residual capacity (FRC) of 3.3 × 10^3 m^3.

[c] Unnumbered because of imprecise information.

[d] Previous ICRP Model.

• As described in the text, lymph nodes are located only in BB region but drain the broncholar and alveolar interstitial regions as well as the bronchial region.

evaluate the different available dosimetry models; to appreciate why they are constructed differently, and to determine which are the most appropriate for extrapolation of the available toxicity data. The section discusses the major factors controlling the disposition of inhaled particles. Note that disposition is defined as encompassing the processes of deposition, absorption, distribution, metabolism, and elimination.

It must be emphasized that dissection of the factors that control inhaled dose into discrete topic discussions is deceptive and masks the dynamic and interdependent nature of the intact respiratory system. For example, although deposition in a particular respiratory region will be discussed separately from the clearance mechanisms for that region, retention (the actual amount of inhaled agent found in the respiratory tract at any time) is determined by the relative rates of deposition and clearance. Retention and the toxicologic properties of the inhaled agent are related to the magnitude of the pharmacologic, physiologic, or pathologic response. Therefore, although the deposition mechanisms, clearance mechanisms, and physicochemical characteristics of particles are described in distinct sections, assessment of the overall dosimetry and toxic response requires integration of the various factors.

Inasmuch as particles which are too massive to be inhaled occur in the environmental air, the description "inhalability" has been used to denote the overall spectrum of particle sizes which are potentially capable of entering the respiratory tract of humans and depositing therein. Except under conditions of microgravity (spaceflight) and possibly some other rare circumstances, unit density particles >100 μm diameter have a low probability of entering the mouth or nose in still air. Nevertheless, there is no sharp cutoff to zero probability because air velocities into the nose or mouth during heavy breathing, or in the presence of a high wind, may be comparable to the settling velocity of >100-μm particles. Even though the settling velocity of particles of this size is >25 cm/s, wind velocities of several m/s can result in them being blown into the nose or mouth. Inhalability can be defined as the ratio of the number concentration of particles of a certain aerodynamic diameter, d_{ae}, that are inspired through the nose or mouth to the number concentration of the same d_{ae} present in the inspired volume of ambient air (ICRP66, 1994). The concept of aerodynamic diameter is discussed in Section 10.2. In studies with head and torso models, inhalability has been considered generally under conditions of different wind velocities and horizontal head orientations.

The American Conference of Governmental Industrial Hygienists (ACGIH) (1985) expressed inhalability in terms of an intake efficiency of a hypothetical sampler. This expression was replaced in 1989 by international definitions for inspirable (also called inhalable), thoracic, and respirable fractions of airborne particle (Soderholm, 1989). Agreement on these definitions has been achieved between the International Standards Organization (ISO) and the ACGIH (Vincent, 1995). Health-related sampling should be based on one or more of the three, progressively very-finer, particle size-selective fractions; inhalable, thoracic, and respirable.

Each definition is expressed as a sampling efficiency (S) which is a function of particle aerodynamic diameter (d_{ae}) and specifies the fraction of the ambient concentration of airborne particles collected by an ideal sampler. For the inspirable fraction,

$$\mathbf{SI}(d_{ae}) = 0.5(1 + e^{-0.06 d_{ae}}). \qquad (10\text{-}4)$$

For the thoracic fraction,

$$\mathbf{ST}(d_{ae}) = \mathbf{SI}(d_{ae})\,[1 - F(x)], \qquad (10\text{-}5)$$

where

$$F(x) = \frac{\ln(d_{ae}/\Gamma)}{\ln(\Sigma)},\ \Gamma = 11.64\ \mu m,\ \Sigma = 1.5. \qquad (10\text{-}6)$$

F(x) is the cumulative probability function of a standardized normal random variable. For the respirable fraction,

$$\mathbf{SR}(d_{ae}) = \mathbf{SI}(d_{ae})\,[1 - F(x)], \qquad (10\text{-}7)$$

where

$$\Gamma = 4.25\ \mu m,\ \Sigma = 1.5. \qquad (10\text{-}8)$$

It should be emphasized that these conventions do not purport to reflect deposition per se, but are rather intended to be representative of the penetration of particles to a region and hence their availability for deposition. The thoracic fraction corresponds to penetration to the TB plus A regions, and the respirable fraction to the A region. Inhalability for laboratory animals is discussed in Section 10.5.2.

Swift (1976) estimated the deposition of particles by impaction in the nose, based on a nasal entrance velocity of 2.3 m/s and a nasal entrance width of 0.5 cm, and deduced that particles >61 μm d_{ae} have a negligible probability of entering the nasal passages due to the high impaction efficiency of the external nares. Experiments by Breysse and Swift (1990) in tranquil air estimated a practical upper limit for inhalability to be ~ 40 μm d_{ae} for individuals breathing at 15 breaths per min at rest. No information on tidal volumes was provided. Studies reported by Vincent (1990) of inhalability made use of a mannequin with mouth and nasal orifices that could be placed in a wind tunnel and rotated 360 degrees horizontally. At low wind speeds, the intake efficiency approached 0.5 for particle sizes between 20 μm and 100 μm d_{ae}. Vincent derived the following empirical relationship from these studies

$$\eta_1 \text{ (sampler)} = 0.5\,[1 + \exp(-0.06\, d_{ae}) = 1 \times 10^{-5}\, U^{2.75} \exp(0.055\, d_{ae}), \qquad (10\text{-}9)$$

where η_1 is the intake efficiency of the sampler, d_{ae} is the aerodynamic diameter, and U is the wind speed. For particles with d_{ae} less than about 40 μm, intake efficiency generally tends to decrease with increasing d_{ae}. However, for large particles, the intake efficiency tends to increase with windspeed. For particles with d_{ae} < 10 μm, the ICRP modified Vincent's expression to increase the accuracy in representing the data. Thus, in the 1994 ICRP66 model (ICRP66, 1994) the intake efficiency of the head, η_l, i.e., the particle inhalability, is represented by

$$\eta_1 = 1 - 0.5\,(1 - [7.6 \times 10^{-4}\,(d_{ae})^{2.8} + 1]^{-1}) + 1 \times 10^{-5}\, U^{2.75} \exp(0.055\, d_{ae}), \qquad (10\text{-}10)$$

where d_{ae} is in μm and U is the windspeed in (m s^{-1}) (for $0 \le U \le 10$ ms^{-7}).

While there is some contention about the practical upper size limit of inhalable particles in humans, there is no lower limit to inhalability as long as the particle exceeds a critical

(Kelvin) size where the aggregation of atomic or molecular units is stable enough to endow it with "particulate" properties, in distinction to those of free ions or gas molecules. *Inter alia,* particles are considered to experience inelastic collisions with surfaces and with each other. The lower limit for the existence of aerosol particles is assumed to be around 1 nanometers for some materials (refer to Section 10.2.). If the particulate material has an appreciable vapor pressure, particles of a certain size may "evaporate" as fast as they are formed. For example, pure water droplets as large as 1 μm diameter will evaporate in less than 1 second even when they are in water-saturated air at 20° Celsius (Greene and Lane, 1957).

Description of a "respirable dust fraction" was first suggested by the British Medical Research Council and implemented by C.N. Davies (1952) using the experimentally-estimated alveolar deposition curve of Brown et al. (1950). This curve described the respirable dust fraction as that which would be available to deposit in the alveolated lung structures including the respiratory bronchioles, thereby making "respirable dusts" applicable to pneumoconiosis-producing dusts. The horizontal elutriator was chosen as a particle size selector, and respirable dust was defined as that dust passing an ideal horizontal elutriator. The elutriator cutoff was chosen to result in the best agreement with experimental lung deposition data. The Johannesburg International Conference on Pneumoconiosis in 1959 adopted the same standard (Orenstein, 1960). Later, an Atomic Energy Commission working group defined "respirable dust" by a deposition curve which indicated 0% deposition at 10 μm d_{ae} and 100% deposition for particles $\leq$2.0 μm d_{ae}. "Respirable dust" was defined as that portion of the inhaled dust which penetrates to the nonciliated portions of the lung (Hatch and Gross, 1964). The AEC respirable size deposition curve was pragmatically adjusted to 100% deposition for $\leq$2 μm d_{ae} particles so that the "respirable" curve could be approximated by a two-stage selective sampler and because comparatively little dust mass was represented by these small particles (Mercer 1973a). This definition was not intended to be applicable to dusts that are readily soluble in body fluids or are primarily chemical intoxicants, but rather only for poorly soluble particles that exhibit prolonged retention in the lung.

Other groups, such as the American Conference of Governmental Industrial Hygienists (ACGIH), incorporated respirable dust sampling concepts in setting acceptable exposure levels for other toxic dusts. Such applications are more complicated, since laboratory animal

and human exposure data, rather than predictive calculations, form the data base for standards. The size-selector characteristic specified in the ACGIH standard for respirable dust (Threshold Limits Committee, 1968) was almost identical to that of the AEC, differing only at 2 μm d_{ae}, where it allowed for 90% passing the first-stage collector instead of 100 percent. The difference between them appeared to be a recognition of the properties of real particle separators, so that, for practical purposes, the two standards could be considered equivalent (Lippmann, 1978).

The cutoff characteristics of the precollectors preceding respirable dust samplers are defined by these criteria. The two sampler acceptance curves have similar, but not identical, characteristics, due mainly to the use of different types of collectors. The BMRC curve was chosen to give the best fit between the calculated characteristics of an ideal horizontal elutriator and available lung deposition data; on the other hand, the design for the AEC curve was based primarily on the upper respiratory tract deposition data of Brown et al. (1950). The separation characteristics of cyclone type collectors simulate the AEC curve. Whenever the particle size distribution has a $\sigma_g > 2$, samples collected with instruments meeting either criterion will be comparable (Lippmann, 1978). Various comparisons of samples collected on the basis of the two criteria are available (Knight and Lichti, 1970; Breuer, 1971; Maquire and Barker, 1969; Lynch, 1970; Coenen, 1971; Moss and Ettinger, 1970).

The various definitions of respirable dust were somewhat arbitrary, with the BMRC and AEC definitions being based on the poorly soluble particles that reach the A region. Since part of the aerosol that penetrates to the alveoli remains suspended in the exhaled air, respirable dust samples are not intended to be a measure of A deposition but only a measure of aerosol concentration for those particles that are the primary candidates for A deposition. Given that the "respirable" dust standards were intended for "insoluble dusts", most of the samplers developed to satisfy their criteria have been relatively simple two-stage instruments. In addition to an overall size-mass distribution curve, multistage aerosol sampler data can provide estimates of the "respirable" fraction and deposition in other functional regions. Field application of these samplers has been limited because of the increased number and cost of sample analyses and the lack of suitable instrumentation. Many of the various samplers, along with their limitations and deficiencies, were reviewed by Lippmann (1978).

PM_{10} dust is based on the PM10 sampler efficiency curve promulgated by the U.S. Environmental Protection Agency. This sample is equivalent to the thoracic dust sample defined by the American Conference of Governmental Industrial Hygienists (Raabe, 1984).

The medical field also refers to a "respirable fraction". Aerosols are widely used for both therapy and diagnosis (Swift, 1993). Aerosols are used to deliver bioactive substances to the respiratory tract to affect a physiological change (e.g., nasal or bronchial medication), provocation tests in the diagnosis of bronchial asthma, and the administration of contrast substances for radiological studies. In pharmaceutical applications, the "respirable fraction" refers to particles with an aerodynamic diameter between 0.5 and 5 μm for most therapeutic products, although larger size particles (up to 10 μm) are recognized as important in certain situations (Hallworth, 1993; Lourenco and Cotromanes, 1982). Aerosols produced by metered-dose-inhaler (MDI) systems are about 2.5 to 2.8 μm in size upon entering the lung (Kim et al., 1985) and 40 to 50% of these aerosols are expected to deposit during normal tidal breathing. The lung deposition, however, is usually higher in the abnormal lung, and can be further increased by changing the mode of breathing.

10.4.1 Deposition Mechanisms

This section will review briefly the aerosol physics that both explains how and why particle deposition occurs and provides the theoretician a capability to develop predictive deposition models. Some of these models will be described in Section 10.5, together with recent experimental results on particle deposition. The ability of the experimentalist to measure deposition quantitatively has continued to advance, but theoretical models remain the only practical way for predicting the impact of aerosol exposures and for delineating the patterns of intra-regional deposition.

The motion of an airborne particle between 1 and 100 µm d_{ae} is primarily related to its mass, and the resulting resistive force of air which is proportional to

$$\mu v d, \qquad (10\text{-}11)$$

where µ is the viscosity of air, v is the velocity of the particle relative to the air, and d is the particle diameter. This is a statement of Stokes law for viscous resistance which is

appropriate to a sphere moving in air at low particle Reynolds numbers, i.e., less than 1. The particle Reynolds number (Re_p) is defined as

$$\rho_a dv/\mu, \qquad (10\text{-}12)$$

where ρ_a is the density of air. When the particle velocity relative to air is sufficiently slow that the airflow pattern around the sphere is symmetrical and only viscous stresses resist the sphere's motion, Stokes law applies. As the value of Re_p increases, asymmetrical flow about the moving sphere and a pressure drop across the sphere, both progressively develop. These changes in flow signify that the condition of inertial resistance prevails and Stokes law does not pertain (Mercer, 1973b).

For the range of particle sizes just discussed (1 to 100 µm), the motion of airborne particles is characterized by a rapid attainment of a constant velocity whereby the viscous resistance of air matches the force(s) on the sphere responsible for its motion. This constant velocity is termed the terminal velocity of the particle. For the size region below 1 µm diameter, particle motion is also based on the viscous resistance of air and described by its terminal velocity. In this particle size region, the viscous resistance of air on the particle, using Stokes law, begins to be overestimated and the particle's terminal velocity, underestimated. This general phenomenon is termed "slip"; consequently, Slip Correction Factors have been developed. These slip corrections become more important as the particle diameter nears, or is less than, the mean free path of air molecules ($\approx$ 0.068 μm at 25 °C and 760 mm Hg air pressure).

10.4.1.1 Gravitational Settling or Sedimentation

All aerosol particles are continuously influenced by gravity, but for practical purposes, particles with an $d_{ae} > 0.5$ µm are mainly involved. Within the respiratory tract, an d_{ae} of 100 µm will be considered as an upper cut-off. A spherical, compact particle within these arbitrary limits will acquire a terminal settling velocity when a balance is achieved between the acceleration of gravity, g, acting on the particle of density, ρ, (g/cm^3) and the viscous resistance of the air according to Stokes law

$$(\pi/6)\rho d^3 g = 3\pi\mu d v_t. \quad (10\text{-}13)$$

The left hand side of Equation 10-13 is the force of gravity on the particle, neglecting the effect of the density of air. Solving for the terminal velocity, v_t, gives

$$v_t = d_{ae}^2 \rho g K_s / 18\mu. \quad (10\text{-}14)$$

In Equation 10-14 a slip correction factor, K_s, is added to account for the slip effect on particles with diameters about or below 1 µm. For particles as small as 0.02 µm, the K_s used by Knudsen and Weber increases v_t six fold (cited by Mercer, 1973c).

The relationship for the terminal settling velocity, just described, is not restricted to measurements in tranquil air. For example, moving air in a horizontal airway will tend to carry the particle at right angles to gravity at an average velocity, U. The action of gravity on the particle will nonetheless result in a terminal settling velocity, v_t; consequently the particle will follow, vectorially, the two velocities; and, provided the airway is sufficiently long or the settling velocity is relatively high, the particle will sediment in the airway. For every orientation of the airways with respect to gravity, it is possible to calculate the particle's settling behavior using Stokes law.

10.4.1.2 Inertial Impaction

Sudden changes in airstream direction and velocity, cause particles to fail to follow the streamlines of airflow as depicted in Figure 10-5. As a consequence, the relatively massive particles impact on the walls or branch points of the conducting airways. The ET and upper TB airways have been described as the dominant sites of high air velocities and sharp directional changes; hence, they dominate as sites of inertial impaction. Because the air (and particle) velocities are affected by the breathing pattern, it is easy to imagine that even small particles also experience some inertial impaction. Moreover, as nasal breathing shifts to oral breathing during work or exercise, the particle that would normally be expected to impact in the ET region will pass into the TB region, greatly increasing TB deposition. That all

impaction sites occur lower down in the TB region when such a shift takes place is also expected.

The probability that a particle with a diameter, d, moving in an air stream with an average velocity, U, will impact at a bifurcation is related to a parameter called the Stokes number, Stk; defined as

$$\rho d^2 U/9\mu D_a , \tag{10-15}$$

or

$$\rho d_{ae}^2 U/9\mu D_a . \tag{10-16}$$

As far as particulate properties are concerned, the aerodynamic diameter (d_{ae}) is again the significant parameter (see Section 10.2). In Landahl's lung deposition model (1950a) of impaction in the TB region, impaction efficiency was proportional to

$$\rho d^2 U_i \sin \theta_i / D_{ai} S_{i-1}, \tag{10-17}$$

where U_i is the air velocity in the airway generation i, θ_i is the branching angle between generations i and i-1, D_{ai} is diameter of the airway of generation i, and S_{i-1} is the total cross sectional area of airway generation i-1.

Prevailing TB models have simplistically represented the airways as smooth, bifurcating tubes. Martonen et al. (1993; 1994a,b,c) have predicted that the cartilaginous rings and carinal ridges perturb the dynamics of airflow and help to explain the non-uniformity of particle deposition.

It should be evident that both gravitational settling and inertial impaction cause the deposition of many particles within the same size range. These deposition forces are always acting together in the ET and TB regions, with inertial impaction dominating in the upper airways and gravitational settling becoming increasingly dominant in the lower conducting

airways, and especially for the largest of the particles which can penetrate into the transitional airways and alveolar spaces.

For sedimenting particles with diameters between 0.1 μm to 1.0 μm, their Slip Correction Factor will be greater than 1.0, although the magnitude of their respective v_t will only range from about 1 μm/s to 35 μm/s. Concurrently, 0.1 μm diameter particles are affected by diffusion such that the root mean displacement they experience in one second is about 0.3 μm. The size region, 1.0 μm down to about 0.1 μm, is frequently described as consisting of particles which are too small to settle and too large to diffuse. Indeed, it is this circumstance that makes them the most persistent and stable particles in aerosols and those which undergo the least deposition in the respiratory tract. As any aerosol ages and continuously undergoes deposition without particle replenishment, the ultimate aerosol will exist largely within this same size range, i.e., have a median size of about 0.5 μm diameter.

10.4.1.3 Brownian Diffusion

Particles <1 μm diameter are increasingly subjected to diffusive deposition as their size decreases. Even particles in the nanometer diameter range are large compared to individual air molecules, hence, the collisions resulting between air molecules, undergoing random thermal motion, and the surface of a particle produce numerous very small changes in the particle's spatial position. These frequent, minute excursions are each made at a constant or terminal velocity due to the viscous resistance of air. The root mean square (r.m.s.) displacement that the particle experiences in a unit of time along a given cartesian coordinate, x, y or z is a measure of its diffusivity. For instance, a 0.1 μm diameter particle has a r.m.s. displacement of about 37 μm during one s. This 1 μm displacement in one s does not describe a velocity of particle motion because the displacement resulted from numerous relatively high velocity excursions.

The diffusion of particles by Brownian motion is described by the Einstein-Stokes' equation

$$\Delta_x = \sqrt{2Dt}, \qquad (10\text{-}18)$$

where Δ_x is the root-mean-square displacement in one second along coordinate x, *D* is the diffusion coefficient for the particle expressed in cm^2/s, t is time in seconds. The diffusion coefficient of a particle of diameter, d, is

$$D = \kappa T K_s / 3\pi\mu d, \qquad (10\text{-}19)$$

where κ is the Boltzmann constant, and T the absolute temperature, collectively describing the average kinetic energy of the gas molecules.

It is apparent that the density of the particle is ordinarily unimportant in determining particle diffusivity which increases as K_s increases and d decreases. Instead of having an aerodynamic equivalent size, diffusive particles of different shapes can be related to the diffusivity of a thermodynamic equivalent size based on spherical particles (Heyder and Scheuch, 1983). In terms of the architecture of the respiratory tract, diffusive deposition of particles is favored by proximate surfaces and by relatively long residence times for particles, both conditions occurring in the alveolated structures of the lungs, the A region. Experimental studies with diffusive particles (<0.5 μm) in replicate casts of the human nose and theoretical predictions both indicate a rising deposition efficiency for the nasal airways as d becomes very small (Cheng et al., 1988).

10.4.1.4 Interception

The interception potential of any particle depends on its physical size. As a practical matter, particles that approach sizes > 150 μm or more in one dimension will be too massive to be inhaled. Airborne fibers (length/diameter ≥ 3), however, frequently exceed 150 μm in length and appear to be relatively stable in air. This is because their aerodynamic size is determined predominantly by their diameter, not their length. Fibers, therefore, are the chief concern in the interception process, especially as their length approaches the diameters of peripheral airways (>150 μm).

The theoretical model of Asgharian and Yu (1988, 1989) for the deposition of fibrous particles in the respiratory tract is complex. While the model includes interception as an important process for long fibers, it also depends on a combination of inertial, gravitational

and diffusional forces to explain fiber deposition. The deposition efficiencies of the three deposition mechanisms cited have been developed for spherical particles, but these can be extended to fibrous particles by considering orientation effects which are strongly related to the direction of airflow. The orientation of fibers depends upon the velocity shear of the airflow and Brownian motion.

For their analysis of orientational effects throughout the respiratory tract, Asgharian and Yu (1988, 1989) defined the equivalent mass diameter, d_{em}, of fibers as

$$d_{em} = d_f \, \beta^{1/3}, \tag{10-20}$$

where d_f is the fiber diameter and β is its aspect ratio (length/diameter). For example, a fiber 100 μm long and 3 μm diameter has a d_{em} of 10 μm diameter. In Figure 10-8, two sets of TB deposition predictions for the rat are reproduced from Asgharian and Yu (1989) that clearly show an example of the relative importance of particle interception.

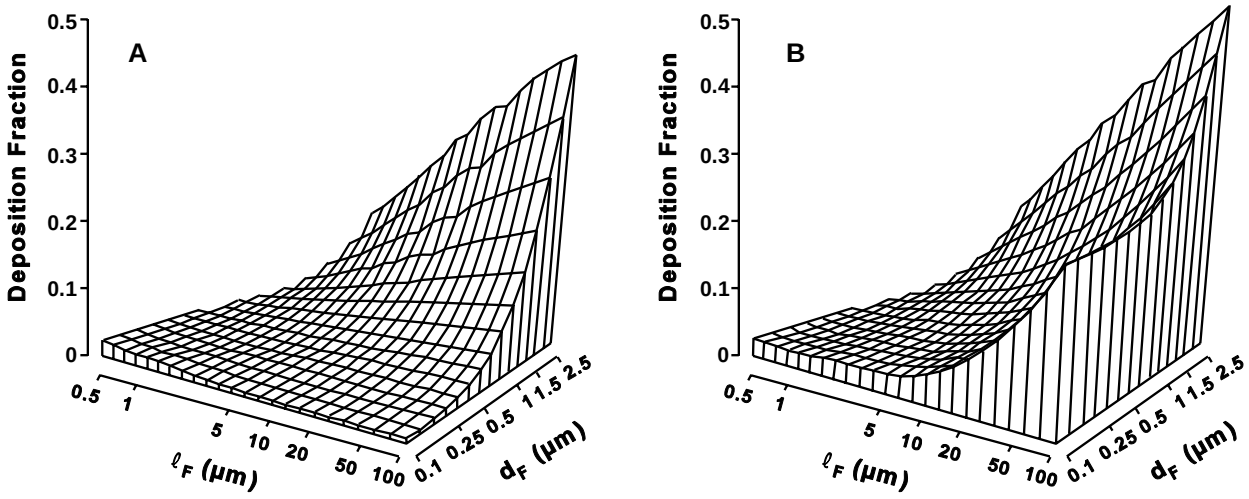

Figure 10-8. Estimated tracheobronchial (TB) deposition in the rat lung, via the trachea, with no interceptional deposition. Graph A is shown in relation to total TB deposition, via the trachea; Graph B for the same fibrous aerosol under identical respiratory conditions including interception.

Source: Asgharian and Yu (1989).

Several general reviews of particle deposition mechanisms in the human respiratory tract have been published, e.g, Stuart (1973), Lippmann (1977), and Brain and Blanchard (1993), and are recommended to the reader, as is the excellent review of particle deposition mechanisms prepared by Phalen (1984).

10.4.1.5 Electrostatic Precipitation

The minimum charge an aerosol particle can have is zero, when it is electrically neutral. This condition is rarely achieved because of the random charging of aerosol particles by the omnipresent air ions. Every cubic centimeter of air contains about 10^3 ions in approximately equal numbers of positive and negative ions. Aerosol particles that are initially neutral will acquire charges from these ions by collisions with them due to their random thermal motion. Aerosols that are initially charged will lose their charge slowly as the charged particles attract oppositely charged ions. An equilibrium state of these competing processes is eventually achieved. The Boltzmann equilibrium represents the charge distribution of an aerosol in charge equilibrium with bipolar ions. The minimum amount of charge is very small, with a statistical probability that some particles will have no charge and others will have one or more charges.

The electrical charge on some particles may result in an enhanced deposition over what would be expected from size alone. This is due to image charges induced on the surface of the airway by these particles or to space-charge effects whereby repulsion of particles containing like charges results in increased migration toward the airway wall. The effect of charge is inversely proportional to particle size and airflow rate. This deposition is probably small compared to the effects of turbulence and other deposition mechanisms and is generally a minor contributor to overall particle deposition, but it may be important in some laboratory studies. This deposition is also negligible for particles below 0.01 μm because so few of these particles carry any charge at Boltzmann equilibrium.

Many of freshly generated particles are electrostatically charged. Experimental studies in a lung cast (Chan et al., 1978) and measurements in rats and humans (Melandri et al., 1977, 1983; Tarroni et al., 1980; Jones et al., 1988; Scheuch et al., 1990) all showed that particle charge increased deposition. For low particle number concentration ($<10^5$ cm^{-3}), the deposition increase is due to the presence of electrostatic image force acting on the

particle by particle-wall interaction (Yu, 1985). Figure 10-8 shows the experimental data on human deposition of Melandri et al. (1983) and Tarroni et al. (1980) for three particle sizes and the modeling results by Yu (1985). The vertical axis in Figure 10-9 is the deposition increment, defined as

$$\Delta T = (DE - DE_o)/(1 - DE_o), \qquad (10\text{-}21)$$

where DE is total deposition at particle charge level, q, and DE_o is the total deposition of particles at Boltzmann charge equilibrium. As seen for each particle size, deposition increments increase linearly with q. Figure 10-9 also shows that there exists a threshold charge level above which the increase in deposition becomes significant. For 1 μm particles, the threshold charge was estimated to be about 54 elementary charges (Yu, 1985).

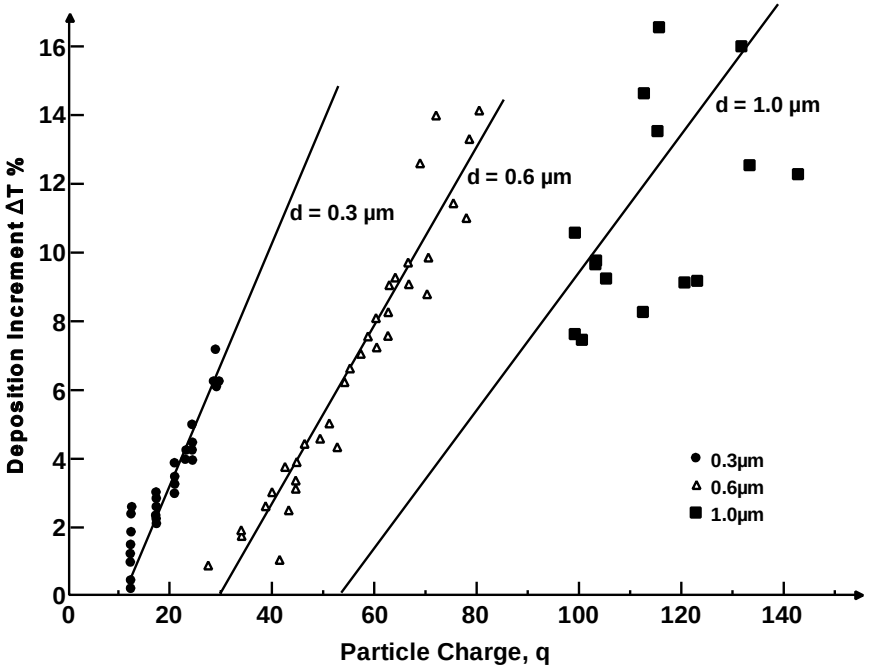

Figure 10-9. Deposition increment data versus particle electronic charge (q) for three particle diameters at 0.3, 0.6, and 1.0 μm (unit density). The solid lines represent the theoretical predictions.

Source: Yu (1985).

10.4.1.6 Additional Factors Modifying Deposition

The available experimental deposition data in humans are commonly for healthy adult Caucasian males using stable, monodisperse particles in charge equilibrium. When these conditions do not hold, changes in deposition are expected to occur. In the following, the effects of different factors on deposition are summarized based upon the information reported from various studies.

Gender

The average size of the adult human femal thorax is smaller than the average thorax size in adult human males. The diameter of the female trachea is approximately 75% that of the male (Warwick and Williams, 1973), and the size of the bronchi is proportional to the size of the trachea (Weibel, 1963). In addition, the minute ventilation and inspiratory flow rate are smaller for females. It is therefore expected that deposition will be different in females than males. Using radioactive-labeled polystyrene particles in the 2.5 to 7.5 μm size range, Pritchard et al. (1986) measured total and regional deposition in 13 healthy nonsmoking female adults at mouth breathing through a tube. Because deposition of particles in this particle size range in the ET region is controlled by impaction, they reported the data as a function of d_{ae}^2 Q to accommodate the difference in flow rate between male and female. The data of Pritchard et al. (1986) for females are shown together with data obtained for a group of male nonsmokers using the same technique in Table 10-4. At a comparative value of d_{ae}^2 Q, females were found to have higher ET and TB deposition and smaller A deposition. The ratio of A deposition to total thoracic deposition in females was also found to be smaller. The differences in depositions were attributed by Pritchard et al. (1986) to the differences in the airway size between males and females.

Age

As a human grows from birth to adulthood, both airway structure and respiratory conditions vary with age. These variations are likely to alter the deposition pattern of inhaled particles. Total deposition data for particles of 1 to 3.1 μm size range were reported by Becquemin et al. (1987, 1991) for a group of 41 children at 5 to 15 years of age and by Schiller-Scotland et al. (1992) for 29 children at two age groups (6.7 and 10.9 years).

TABLE 10-4. DEPOSITION DATA FOR MEN AND WOMEN

Sex	$d_{ae}^2 Q$ (μm^2 $Lmin^{-1}$)	Deposition as a Fraction of Inhaled Material (%) ± Standard Error			
		Total	ET	TB	A
Female	405 ± 47	75.9 ± 1.7	21.2 ± 2.4	16.9 ± 1.5	37.5 ± 2.5
Male	430 ± 41	81.5 ± 1.8	19.9 ± 2.5	14.7 ± 1.7	46.9 ± 2.7

Although Becquemin et al. (1987, 1991) did not find a clear dependence of total deposition on age, slightly higher deposition was found by Schiller-Scotland et al. (1992), for each diameter when children breathed at their normal rates (see Figure 10-10), than was found in adults.

Mathematical models for children have been developed by many workers (Hofmann, 1982; Crawford, 1982; Xu and Yu, 1986; Yu and Xu, 1987; Phalen et al., 1988; Hofmann et al., 1989; Yu et al., 1992; Martonon and Zhang, 1993). Phalen et al. (1988) reported morphometric data of twenty TB airway casts of children and young adults from 21 days to 21 years. With the use of these data, they calculated a higher TB deposition in children during inhalation for particle diameters between 0.01 and 10 µm. If the entire respiratory tract and a complete breathing cycle at normal rate are considered in the model, the results show that ET deposition in children is higher than adults, but that TB and A deposition in children may be either higher or lower than the adult depending upon the particle size (Xu and Yu, 1986).

Respiratory Tract Disease

Effect of airway diseases on deposition have been studied extensively. In 8 healthy nonsmokers, Svartengren et al. (1986, 1989) found A deposition at different flow rates to be lower (26% versus 48% of thoracic deposition) in subjects after induced bronchoconstriction. The degree of bronchoconstriction was quantified by measurements of airway resistance using a whole-body plethysmograph. An inverse relationship between airway resistance and A deposition was found. Data from the same laboratory (Svartengren et al., 1990, 1991) using 2.6 µm d_{ae} particles with maximally deep slow inhalations at 0.5 L/min showed no

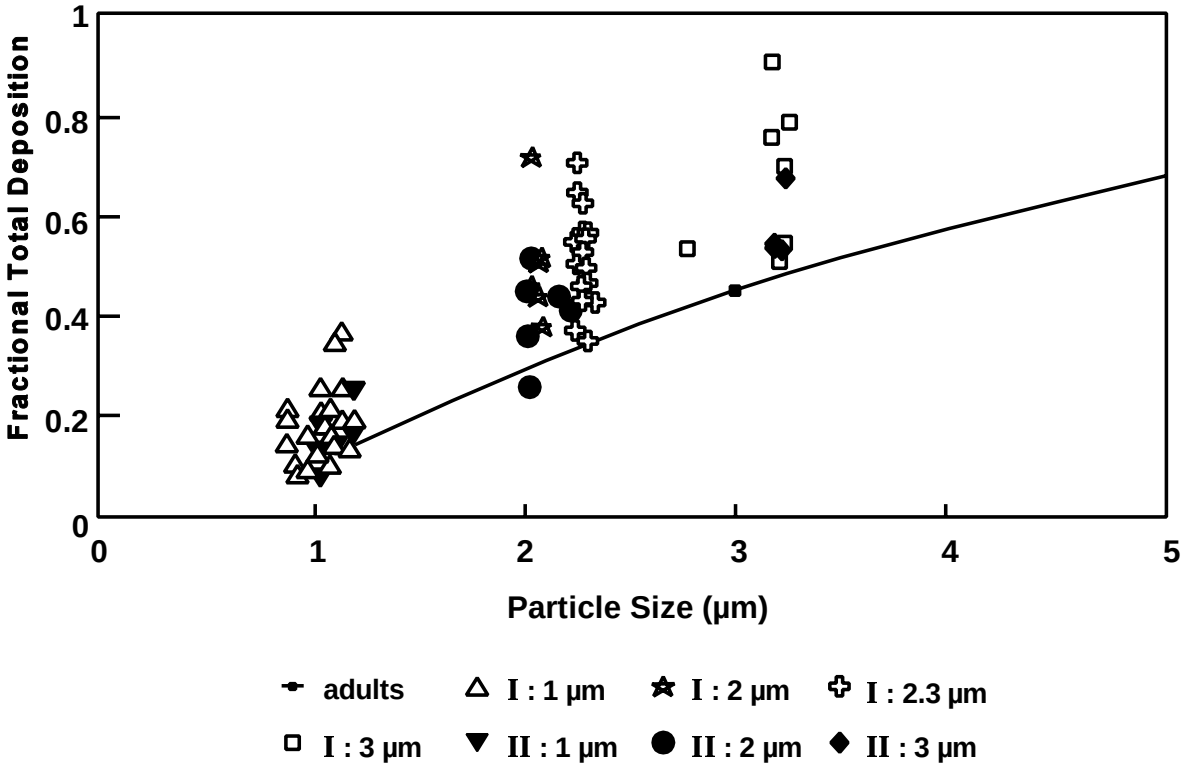

Figure 10-10. Total deposition data in children with or during spontaneous breathing as a function of particle diameter (unit density). Group I (10.6 ± 2.0 yrs); Group II (5.3 ± 1.5 yrs). The adult curve represents the mean value of deposition from the data of Stahlhofen et al. (1989).

Source: Schiller-Scotland et al. (1992).

significant differences in mouth and throat deposition in asthmatics versus healthy subjects, but thoracic deposition was higher in asthmatics than in healthy subjects (83% versus 73% of total deposition). TB deposition was also found to be higher in asthmatics. The results are similar to those found in subjects with obstructive lung disease (e.g., Dolovich et al., 1976; Itoh et al., 1981; Anderson et al., 1990).

Another extensive study of the relationship between deposition and lung abnormality was made by Kim et al. (1988). One-hundred human subjects with various lung conditions (normal, asymptomatic smoker, smoker with small airway disease, chronic simple bronchitis and chronic obstructive bronchitis) breathed 1 µm test particles from a bag at a rate of 30 breaths/min. The number of rebreathing breaths needed to produce a 90% loss of aerosol

from the bag was determined. From these data, they estimated total deposition and found that total deposition increased with increasing level of airway obstruction.

Particle Polydispersity

Aerosol particles are often generated polydisperse and can be approximated by a lognormal distribution (Section 10.2). The mass deposition of spherical particles in the respiratory tract depends upon mass median diameter (MMD), geometric standard deviation, σ_g, and physical density (Diu and Yu, 1983; Rudolf et al., 1988). For large particles (d_{ae} > 1 μm), deposition is governed by impaction and sedimentation. The dependence on MMD and mass density can be combined with the use of mass medium aerodynamic diameter (MMAD), as suggested by TGLD (1966). However, this method is not valid for particles in the size range where diffusion deposition becomes important. Figure 10-11 shows the calculated total and regional mass deposition results by Yeh et al. (1993) for polydisperse aerosols of unit density with various σ_g as function of MMD at quiet mouth breathing. The variation of deposition with σ_g depends strongly on the MMD of the aerosol. At certain MMD's, variability with σ_g is zero; however, variations at other MMD's can be very large. One of the main effects of polydisperse deposition is the flattening of the deposition curves as a function of particle size, as shown in Figure 10-11.

Particle Hygroscopicity

Another important particle factor that affects deposition is the hygroscopicity of the particle. Many atmospheric particles such as acid particles are water soluble. As these particles travel along the humid respiratory tract, they grow in size and, as a result, the deposition pattern is altered. A discussion on deposition of hygroscopic particles follows in Section 10.4.3.

10.4.1.7 Comparative Aspects of Deposition

The various species used in inhalation toxicology studies that serve as the basis for dose-response assessment do not receive identical doses in a comparable respiratory tract region (ET, TB, or A) when exposed to the same aerosol or gas (Brain and Mensah, 1983). Such interspecies differences are important because the adverse toxic effect is likely more

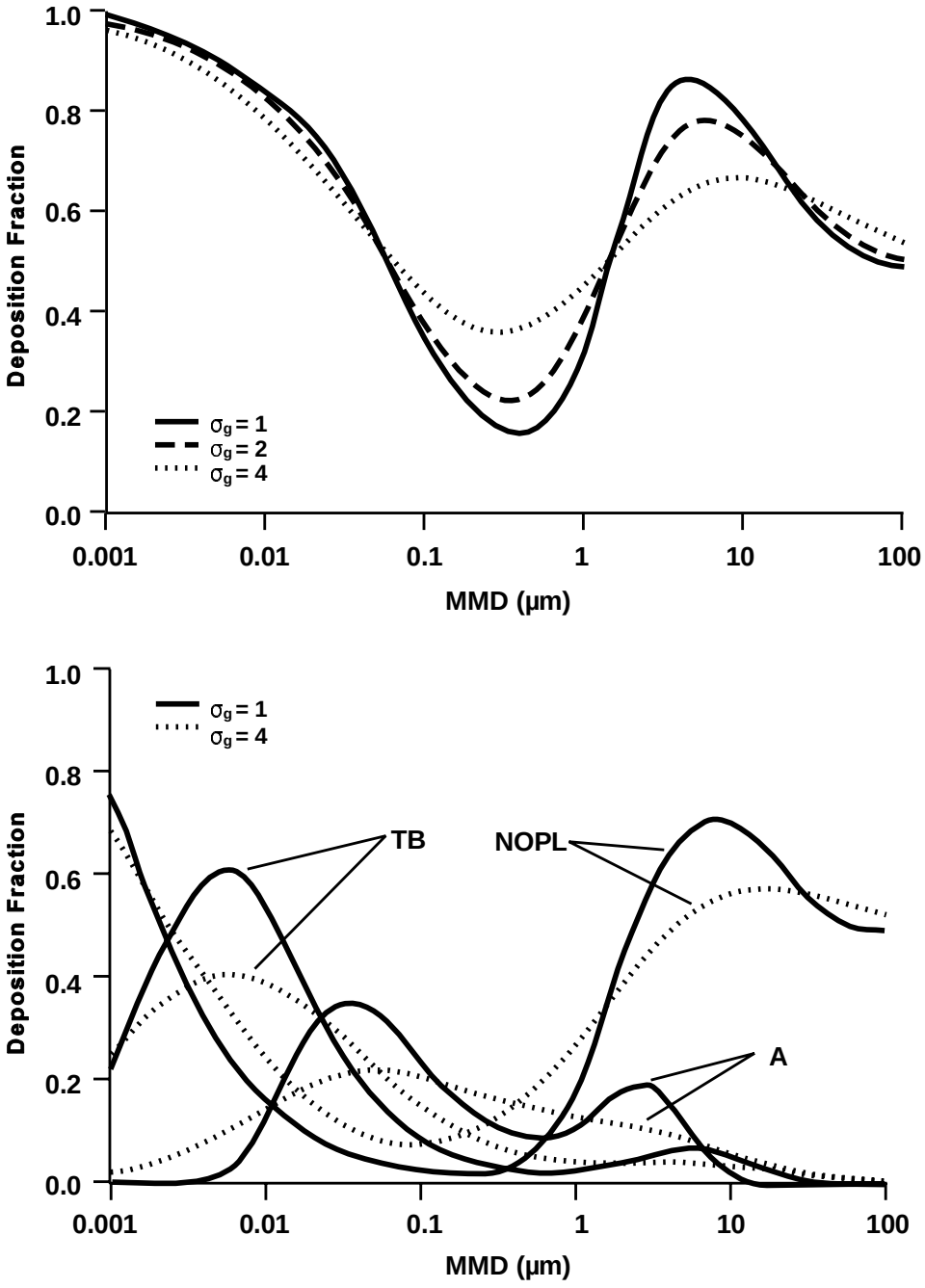

Figure 10-11. Calculated mass deposition from polydisperse aerosols of unit density with various geometric standard deviations (σ_g) as a function of mass median diameter (MMD) for quiet breathing (tidal volume = 750 mL, breathing frequency = 15 min^{-1}). The upper panel is total deposition and the lower panel is regional deposition (NOPL = Naso-oro-pharyngo-laryngeal, TB = Tracheobronchial, A = Alveolar). The range of σ_g values demonstrates the extremes of monodisperse to extremely polydisperse.

Source: Yeh et al. (1993).

related to the quantitative pattern of deposition within the respiratory tract than to the exposure concentration; this pattern determines not only the initial respiratory tract tissue dose but also the specific pathways by which the inhaled material is cleared and redistributed (Schlesinger, 1985b). Differences in ventilation rates and in the URT structure and size and branching pattern of the lower respiratory tract between species result in significantly different patterns of airflow and particle deposition. Disposition varies across species and with the respiratory tract region. For example, interspecies variations in cell morphology, numbers, types, distributions, and functional capabilities contribute to variations in clearance of initially deposited dose. Tables 10-5, 10-6, and 10-7 summarize some of these differences for the ET, TB, and A regions, respectively. This section only briefly summarizes these considerations. Comprehensive and detailed reviews of species differences have been published (Phalen and Oldham, 1983; Patra, 1986; Mercer and Crapo, 1987; Gross and Morgan, 1992; Mercer and Crapo, 1992; Parent, 1992).

The geometry of the upper respiratory tract exhibits major interspecies differences (Gross and Morgan, 1992). In general, laboratory animals have much more convoluted nasal turbinate systems than do humans, and the length of the nasopharynx in relation to the entire length of the nasal passage also differs between species. This greater complexity of the nasal passages, coupled with the obligate nasal breathing of rodents, is generally thought to result in greater deposition in the upper respiratory tract (or ET region) of rodents than in humans breathing orally or even nasally (Dahl et al., 1991), although limited comparative data are available. Species differences in gross anatomy, nasal airway epithelia (e.g., cell types and location) and the distribution and composition of mucous secretory products have been noted (Harkema, 1991; Guilmette et al., 1989). The extent of upper respiratory tract removal affects the amount of particles or gas available to the distal respiratory tract.

Airway size (length and diameter) and branching pattern affect the aerodynamics of the respiratory system in the following ways:

- The airway diameter affects the aerodynamics of the air flow and the distance from the particle to the airway surface.
- The cross-sectional area of the airway determines the airflow velocity for a given volumetric flow.
- Airway length, airway diameter, and branching pattern variations affect the mixing between tidal and residual air.

TABLE 10-5. INTERSPECIES COMPARISON OF NASAL CAVITY CHARACTERISTICS

	Sprague-Dawley Rat	Guinea Pig	Beagle Dog	Rhesus Monkey	Human
Body weight	250 g	600 g	10 kg	7 kg	≈70 kg
Naris cross-section	0.7 mm	2.5 mm^2	16.7 mm^2	22.9 mm^2	140 mm^2
Bend in naris	40°	40°	30°	30°	
Length	23 cm	3.4 cm	10 cm	5.3 cm	7-8 cm
Greatest vertical diameter	9.6 mm	12.8 mm	23 mm	27 mm	40-45 mm
Surface area (both sides of nasal cavity)	10.4 cm^2	27.4 cm^2	220.7 cm^2	61.6 cm^2	181 cm^2
Volume (both sides)	0.4 cm	0.9 cm^3	20 cm^3	8 cm^3	16-19 cm^3 (does not include sinuses)
Bend in nasopharynx	15°	30°	30°	80°	≈90°
Turbinate complexity	Complex scroll	Complex scroll	Very complex membranous	Simple scroll	Simple scroll

[a]Adult male.

Source: Schreider (1983); Gross and Morgan (1992).

TABLE 10-6. COMPARATIVE LOWER AIRWAY ANATOMY AS REVEALED ON CASTS

	Gross Structure					Typical Structure (Generation 6)			
Mammal/ Body Mass	Left Lung Lobes	Right Lung Lobes	Airway Branching	Trachea Length/Diameter (cm)	Major Airway Bifurcations	Average Airway L/D (ratio)	Branch Angles (Major Daughter/ Minor Daughter) (degrees)	Typical Number of Branches to Terminal Bronchiole	Respiratory Bronchioles
Human/70 kg	Upper and lower	Upper, middle, and lower	Relatively symmetric	12/2	Sharp for about the first 10 generations, relatively blunt thereafter	2.2	11/33	14-17	About 3-5 orders
Rhesus monkey/2 kg	Superior, middle, and inferior	Superior, middle, and inferior, azygous	Monopodial	3/0.3	Mixed blunt and sharp	2.6	20/62	10-18	About 4 orders
Beagle dog/ 10 kg	Apical, intermediate, and basal	Apical, intermediate, and basal	Strongly monopodial	17/1.6	Blunt tracheal bifurcation, others sharp	1.3	8/62	15-22	About 3-5 orders
Ferret/ 0.61 kg	NR[a]	NR	strongly monopodial	10/0.5	Sharp	2.0	16/57	12-20	About 3-4 orders
Guinea pig/ 1 kg	Superior and inferior	Superior, middle, and inferior	Monopodial	5.7/0.4	Very sharp and high	1.7	7/76	12-20	About 1 order
Rabbit/ 4.5 kg	Superior and inferior	Cranial, middle, caudal, and postcaval	Strongly monopodial	6/0.5	Sharp	1.9	15/75	12-20	About 1-2 orders
Rat/0.3 kg	One lobe	Cranial, middle, caudal, and postcaval	Strongly monopodial	2.3/0.26	Very sharp and very high throughout lung	1.5	13/60	12-20	Rudimentary
Golden hamster/ 0.14 kg	Superior and inferior	Cranial, middle, caudal, and postcaval	Strongly monopodial	2.4/0.26	Very sharp	1.2	15/63	10-18	About 1 order

[a]NR = Not reported.

Source: Phalen and Oldham (1983); Patra (1986); Mercer and Crapo (1987).

TABLE 10-7. ACINAR MORPHOMETRY

Species	Fixation	Number of Acini/Lung[1]	V (mm^3)	D or L (mm)[2]	Number Alveoli/Acinus	Alveolar Duct Generations	References
Human			1.33-30.9		15,000		Pump (1964)
		27,992			10,714	6	Horsfield and Cumming (1968); Parker et al. (1971)
	75% TLC	23,000	160.8	7.04 (L)	14,000-20,000	9	Hansen and Ampaya (1975); Hansen et al. (1975)
		80,000	15.6			2-5	Boyden (1972)
				5.1 (L)	7,100	8-12	Schreider and Raabe (1981)
	TLC	26,000-32,000	187.0	8.8 (L)	10,344	9	Haefeli-Bleuer and Weibel (1988)
	FRC	43,000	51.0	6.0 (D)	8,000	9	Mercer, and Crapo (1992)
Rabbit		17,900	2.54				Kliment (1973)
	55% TLC	18,000	3.46	1.95 (L)		6	Rodriguez et al. (1971)
Guinea pig		5,100	1.25				Kliment (1973)
	FRC	4,097	1.09	1.56 (D)	6,890	9-12	Mercer and Crapo (1992)
Rat		2,500	1.0				Kliment (1973)
		2,487	5.06				Yeh et al. (1979)
	FRC	2,020	1.9	1.5 (D)	5,243	10-12	Mercer et al., 1987
	70% TLC	5,993	1.46	1.5 (L)		6	Rodriguez et al. (1987)

[1]Volume of lung at fixation (TLC, total lung capacity; FRC, functional residual capacity).
[2]Acinar size (D, diameter; L, length).

Source: Mercer and Crapo (1992).

The airways show a considerable degree of variability within species (e.g., size and branching pattern) and this is most likely the primary factor responsible for the deposition variability seen within single species (Schlesinger, 1985a).

Larger airway diameter results in greater turbulence for the same relative flow velocity (e.g., between a particle and air). Therefore, flow may be turbulent in the large airways of humans, whereas for an identical flow velocity, it would be laminar in the smaller laboratory animal. Relative to humans, laboratory animals also tend to have tracheas that are much longer in relation to their diameter. This could result in increased relative deposition in humans because of the increased likelihood of laryngeal jet flow extending into the bronchi. Human airways are characterized by a more symmetrical dichotomous branching than that found in most laboratory mammals, which have highly asymmetrical airway branching (monopodial). The more symmetrical dichotomous pattern in humans is susceptible to deposition at the carina because of its exposure to high air flow velocities toward the center of the air flow profile.

Alveolar size also differs between species, which may affect deposition efficiency due to variations on the distance between the airborne particle and alveolar walls (Dahl et al., 1991).

Addressing species differences in ventilation, which affects the tidal volume and ventilation to perfusion ratios, is also critical to estimating initial absorbed dose. Due to the expected variations in airflows within the respiratory tract, the variability among lungs in the human or laboratory animal population, and the variations in respiratory performance that members of the population experience during their normal activities, e.g. sleep and exercise, must be considered in order to gain some insight into the variability that might be expected in particle deposition, total and regional, of particles in the urban atmosphere. The experimentalist must try to keep respiratory parameters relatively constant to obtain reasonably consistent deposition data.

10.4.2 Clearance and Translocation Mechanisms

Particles that deposit upon airway surfaces may be cleared from the respiratory tract completely, or may be translocated to other sites within this system, by various regionally distinct processes. These clearance mechanisms, which are outlined in Table 10-8, can be

TABLE 10-8. OVERVIEW OF RESPIRATORY TRACT PARTICLE CLEARANCE AND TRANSLOCATION MECHANISMS

Extrathoracic region
Mucociliary transport
Sneezing
Nose wiping and blowing
Dissolution (for "soluble" particles) and absorption into blood
Tracheobronchial region
Mucociliary transport
Endocytosis by macrophages/epithelial cells
Coughing
Dissolution (for "soluble" particles) and absorption into blood
Alveolar region
Macrophages, epithelial cells
Interstitial
Dissolution for "soluble" and "insoluble" particles (intra-and extracellular)

Source: Schlesinger (1995).

categorized as either absorptive (i.e., dissolution) or nonabsorptive (i.e., transport of intact particles) and may occur simultaneously or with temporal variations. It should be mentioned that particle solubility in terms of clearance refers to solubility within the respiratory tract fluids and cells. Thus, an "insoluble" particle is considered to be one whose rate of clearance by dissolution is insignificant compared to its rate of clearance as an intact particle. For the most part, all deposited particles are subject to clearance by the same mechanisms, with their ultimate fate a function of deposition site, physicochemical properties (including any toxicity), and sometimes deposited mass or number concentration. Clearance routes from the various regions of the respiratory tract are schematically outlined in Figures 10-12 and 10-13. Furthermore, clearance is a continuous process and all mechanisms operate simultaneously for deposited particles.

10.4.2.1 Extrathoracic Region

The clearance of insoluble particles deposited in the nonolfactory portion of nasal passages occurs via mucociliary transport, and the general flow of mucus is backwards, i.e., towards the nasopharynx (Figure 10-12). However, the epithelium of the most anterior portion of the nasal passages is not ciliated, and mucus flow just distal to this is forward,

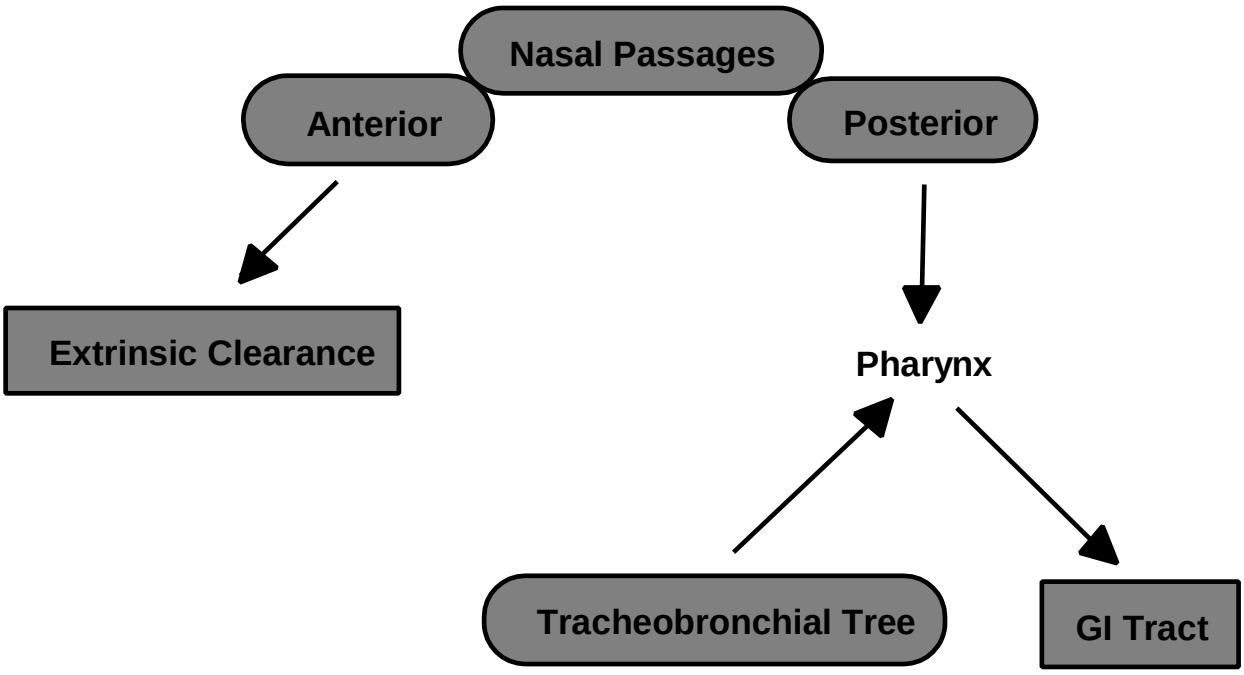

Figure 10-12. Major physical clearance pathways from the extrathoracic region and tracheobronchial tree.

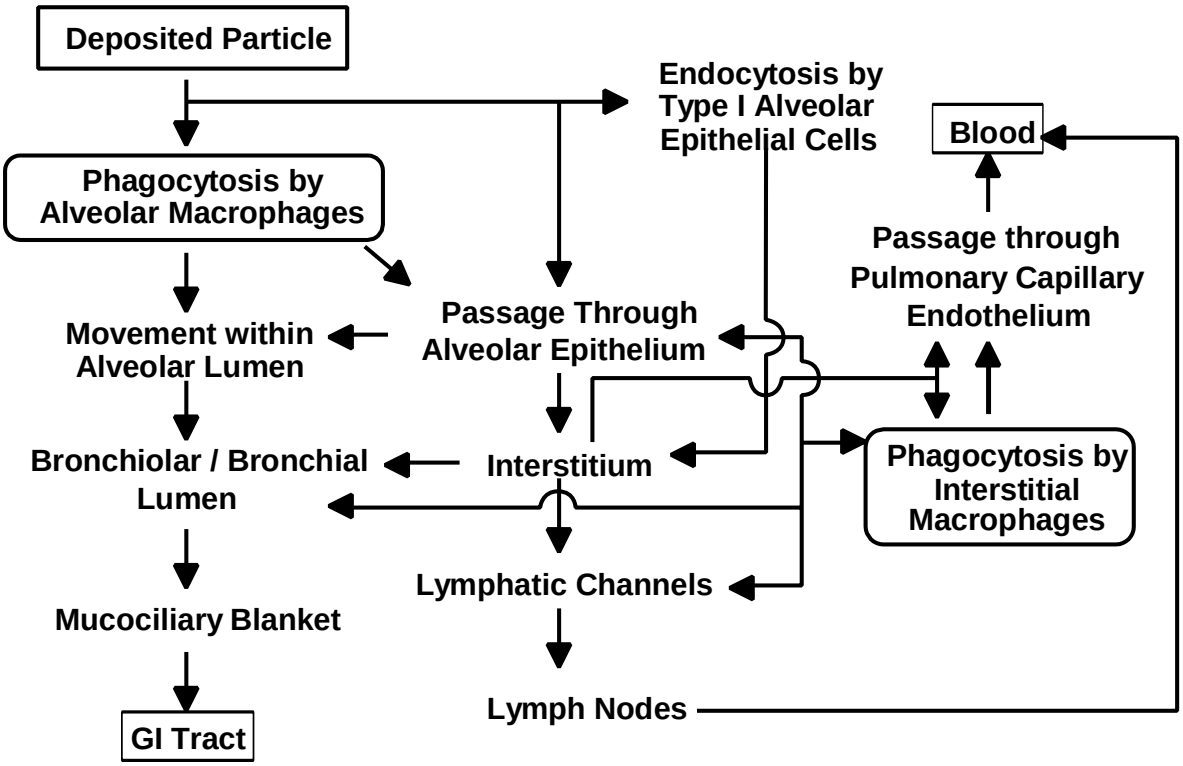

Figure 10-13. Diagram of known and suspected clearance pathways for poorly soluble particles depositing in the alveolar region.

Source: Modified from Schlesinger (1995).

clearing deposited particles to a site (vestibular region) where removal is by sneezing (a reflex response), wiping, or blowing (mechanisms known as extrinsic clearance).

Soluble material deposited on the nasal epithelium will be accessible to underlying cells if it can diffuse to them through the mucus prior to removal via mucociliary transport. Dissolved substances may be subsequently translocated into the bloodstream following movement within intercellular pathways between epithelial cell tight junctions or by active or passive transcellular transport mechanisms. The nasal passages have a rich vasculature, and uptake into the blood from this region may occur rapidly.

Clearance of poorly soluble particles deposited in the oral passages is by coughing and expectoration or by swallowing into the gastrointestinal tract. Soluble particles are likely to be rapidly absorbed after deposition (Swift and Proctor, 1988).

10.4.2.2 Tracheobronchial Region

Poorly soluble particles deposited within the tracheobronchial tree are cleared primarily by mucociliary transport, with the net movement of fluid towards the oropharynx, followed by swallowing. Some poorly soluble particles may traverse the epithelium by endocytotic processes, entering the peribronchial region (Masse et al., 1974; Sorokin and Brain, 1975). Clearance may also occur following phagocytosis by airway macrophages, located on or beneath the mucous lining throughout the bronchial tree. They then move cephalad on the mucociliary blanket, or via macrophages which enter the airway lumen from the bronchial or bronchiolar mucosa (Robertson, 1980).

As in the nasal passages, soluble particles may be absorbed through the mucous layer of the tracheobronchial airways and into the blood, via intercellular pathways between epithelial cell tight junctions or by active or passive transcellular transport mechanisms.

The bronchial surfaces are not homogeneous; there are openings of daughter bronchi and islands of non-ciliated cells at bifurcation regions. In the latter, the usual progress of mucous movement is interrupted, and bifurcations may be sites of relatively retarded clearance. The efficiency with which such non-ciliated regions are traversed is dependent upon the traction of the mucous layer.

Another method of clearance from the tracheobronchial region, under some circumstances, is cough, which can be triggered by receptors located in the area from the

trachea through the first few bronchial branching levels. While cough is generally a reaction to some inhaled stimulus, in some cases, especially respiratory disease, it can also serve to clear the upper bronchial airways of deposited substances by dislodging mucus from the airway surface.

10.4.2.3 Alveolar Region

Clearance from the alveolar (A) region occurs via a number of mechanisms and pathways, but the relative importance of each is not always certain and may vary between species.

Particle removal by macrophages comprises the main nonabsorptive clearance process in the A region. Alveolar macrophages reside on the epithelium, where they phagocytize and transport deposited material. They come into contact with phagocytized material by random motion, or more likely via directed migration under the influence of local chemotactic factors (Warheit et al, 1988). Contact may be facilitated as some deposited particles are translocated, due to pressure gradients or via capillary action within the alveolar surfactant lining, to sites where macrophages congregate (Schurch et al., 1990; Parra et al., 1986).

Alveolar macrophages normally comprise ≈3 - 5% of the total alveolar cells in healthy (non-smoking) humans and other mammals, and represent the largest subpopulation of nonvascular macrophages in the respiratory tract (Gehr, 1984; Lehnert, 1992). However, the actual cell count may be altered by particle loading. While a slight increase of deposited particles may not result in an increase in cell number, macrophage numbers will increase proportionally to particle number until some peak accumulation is reached (Adamson and Bowden, 1981; Brain, 1971). Since the magnitude of this increase is related more to the number of deposited particles than to total deposition by weight, equivalent masses of an identically deposited substance would not produce the same response if particle sizes differed; thus, deposition of smaller particles would tend to result in a greater elevation in macrophage number than would larger particle deposition.

Particle-laden macrophages may be cleared from the A region along a number of pathways (Figure 10-13). One route is cephalad transport via the mucociliary system after the cells reach the distal terminus of the mucus blanket. However, the manner by which macrophages actually reach the ciliated airways is not certain. The possibilities are chance

encounter; passive movement along the alveolar surface due to surface tension gradients between the alveoli and conducting airways; directed locomotion along a gradient produced by chemotactic factors released by macrophages ingesting deposited material; or passage through the alveolar epithelium and the interstitium, perhaps through aggregates of lymphoid tissue known as bronchus associated lymphoid tissue (BALT) located at bronchoalveolar junctions (Sorokin and Brain, 1975; Kilburn, 1968; Brundelet, 1965; Green, 1973; Corry et al., 1984; Harmsen et al., 1985).

Some of the cells which follow interstitial clearance pathways are likely resident interstitial macrophages that have ingested particles which were transported through the alveolar epithelium, probably via endocytosis by Type I pneumocytes (Brody et al., 1981; Bowden and Adamson, 1984). Particle-laden interstitial macrophages can also migrate across the alveolar epithelium, becoming part of the alveolar macrophage cell population (Adamson and Bowden, 1978).

Macrophages that are not cleared via the bronchial tree may actively migrate within the interstitium to a nearby lymphatic channel or, along with uningested particles, be carried in the flow of interstitial fluid towards and into the lymphatic system (Harmsen et al., 1985). Passive entry into lymphatic vessels is fairly easy, since the vessels have loosely connected endothelial cells with wide intercellular junctions (Lauweryns and Baert, 1974). Lymphatic endothelium may also actively engulf particles from the surrounding interstitium (Leak, 1980). Particles within the lymphatic system may be translocated to tracheobronchial lymph nodes, which often become reservoirs of retained material. Particles penetrating the nodes and subsequently reaching the post-nodal lymphatic circulation may enter the blood.

Uningested particles or macrophages in the interstitium may traverse the alveolar-capillary endothelium, directly entering the blood (Raabe, 1982; Holt, 1981); endocytosis by endothelial cells followed by exocytosis into the vessel lumen seems, however, to be restricted to particles $<0.1\ \mu$m diameter, and may increase with increasing lung burden (Lee et al., 1989; Oberdörster, 1988). Once in the systemic circulation, transmigrated macrophages, as well as uningested particles, can travel to extrapulmonary organs. Some mammalian species have alveolar intravascular macrophages, which can remove particles from circulating blood and which may play some role in the clearance of material deposited in the alveoli (Warner and Brain, 1990).

Uningested particles and macrophages within the interstitium may travel to perivenous, peribronchiolar or subpleural sites, where they become trapped, increasing particle burden. The migration and grouping of particles and macrophages within the lungs can lead to the redistribution of initially diffuse deposits into focal aggregates (Heppleston, 1953). Some particles can be found in the pleural space, often within macrophages which have migrated across the visceral pleura (Sebastien et al., 1977; Hagerstrand and Siefert, 1973). Resident pleural macrophages do occur, but their role in clearance, if any, is not certain.

During clearance, particles can be redistributed within the alveolar macrophage population (Lehnert, 1992). This can occur following death of a macrophage, and release of free particles to the epithelium, followed by uptake by other macrophages. Some of these newly freed particles may, however, translocate to other clearance routes.

Clearance by the absorptive mechanism involves dissolution in the alveolar surface fluid, followed by transport through the epithelium and into the interstitium, and diffusion into the lymph or blood. Some soluble particles translocated to and trapped in interstitial sites may be absorbed there. Although the factors affecting the dissolution of deposited particles are poorly understood, solubility is influenced by the particle's surface to volume ratio and other surface properties (Morrow, 1973; Mercer, 1967). Thus, materials generally considered to be relatively insoluble may still have high dissolution rates and short dissolution half-times if the particle size is small.

Some deposited particles may undergo dissolution in the acidic milieu of the phagolysosomes after ingestion by macrophages, and such intracellular dissolution may be the initial step in translocation from the lungs for these particles (Kreyling, 1992; Lundborg et al., 1985). Following dissolution, the material can be absorbed into the blood. Dissolved materials may then leave the lungs at rates which are more rapid than would be expected based upon their normal dissolution rate in lung fluid. For example, while insoluble (in lung fluid) MnO_2 dissolves in the macrophage following ingestion, soluble manganese chloride ($MnCl_2$) likely dissolves extracellularly and is not ingested, resulting in manganese clearing at different initial rates depending upon the form in which it was initially inhaled (Camner et al, 1985). Differences in rates of clearance may also occur for particles whose rate of dissolution is pH dependent (Marafante et al., 1987).

Finally, some particles can bind to epithelial cell membranes or macromolecules, or other cell components, delaying clearance from the lungs.

10.4.2.4 Clearance Kinetics

Deposited particles may be cleared completely from the respiratory tract. However, the actual time frame over which clearance occurs affects the cumulative dose delivered to the respiratory tract, as well as to extrapulmonary organs. Particle-tissue contact and retained dose in the extrathoracic region and tracheobronchial tree are often limited by rapid clearance from these regions. On the other hand, the retained dose from material deposited in the A region is more dependent upon the physicochemical characteristics of the particles.

Various experimental techniques have been used to assess clearance rates in both humans and laboratory animals (Schlesinger, 1985b). Because of technical differences and the fact that measured rates are strongly influenced by the specific methodology, comparisons between studies are often difficult to perform. However, regional clearance rates, i.e., the fraction of the deposit which is cleared per unit time, are well defined functional characteristics of an individual human or laboratory animal when repeated tests are performed under the same conditions; but, as with deposition, there is a substantial degree of inter-individual variability.

Extrathoracic Region

Mucus flow rates in the posterior nasal passages are highly nonuniform. Regional velocities in the healthy adult human may range from < 2 to > 20 mm/min (Proctor, 1980), with the fastest flow occurring in the midportion of the nasal passages. The median rate in a healthy adult human is about 5 mm/min, the net result being a mean anterior to posterior transport time of about 10-20 min for poorly soluble particles deposited within the nasal passages (Stanley et al., 1985; Rutland and Cole, 1981). However, particles deposited in the anterior portion of the nasal passages are cleared more slowly, at a rate of 1-2 mm/h (Hilding, 1963). Since clearance at this rate may take upwards of 12 h, such deposits are usually more effectively removed by sneezing, wiping, or nose blowing, in which case clearance may occur in 0.5 h (Morrow, 1977; Fry and Black, 1973).

Tracheobronchial Region

Mucus transport in the tracheobronchial tree occurs at different rates in different local regions; the velocity of movement is fastest in the trachea, and it becomes progressively slower in more distal airways. In healthy non-smoking humans, and using non-invasive procedures and no anesthesia, average tracheal mucus transport rates have been measured at 4.3 to 5.7 mm/min (Leikauf et al., 1981, 1984; Yeates et al., 1975, 1981b; Foster et al., 1980), while that in the main bronchi has been measured at $\approx$2.4 mm/min (Foster et al., 1980). While rates of movement in smaller airways have not been directly determined, estimates for human medium bronchi range between 0.2-1.3 mm/min, while those in the most distal ciliated airways range down to 0.001 mm/min (Yeates and Aspin, 1978; Morrow et al., 1967b; Cuddihy and Yeh, 1988).

It is not certain whether the transport rate for deposited poorly soluble particles is independent of their nature, i.e., shape, size, composition. While particles of different materials and sizes have been shown to clear at the same rate in the trachea in some studies (Man et al., 1980; Patrick, 1983; Connolly et al., 1978), other studies (using instillation) have indicated that the rate of mucociliary clearance may be greater for smaller particles ($\leq 2\mu$m) than for larger ones (Takahashi et al, 1992). Reasons for such particle-size related differences are not known. There may, however, be more than one phase of clearance within individual tracheobronchial airways. For example, the rat trachea shows a biphasic clearance pattern, consisting of a rapid phase within the first 2-4 h after deposition, clearing up to 90% of deposited particles with a half time of < 0.5 h, followed by a second, slower phase, clearing most of the remaining particles with a half-time of 8-19 h (Takahashi et al, 1992).

The total duration of bronchial clearance, or some other time parameter, is often used as an index of mucociliary kinetics, yet the temporal clearance pattern is not certain. In healthy adult non-smoking humans, 90% of poorly soluble particles depositing within the tracheobronchial tree were found to be cleared from 2.5 to 20 h after deposition, depending upon the individual subject and the size of the particles (Albert et al., 1973). While particle size does not affect surface transport, it does affect the depth of particle penetration and deposition and the subsequent pathway length for clearance. Due to differences in regional transport rates, clearance times from different regions of the bronchial tree will differ.

While removal of a TB deposit is generally 99% completed by 48 h after exposure (Bailey et al., 1985a), there is the possibility of longer-term retention under certain circumstances.

Studies with rodents, rabbits, and humans have indicated that a small fraction ($\approx$1%) of insoluble material may be retained for a prolonged period of time within the upper respiratory tract (nasal passages) or tracheobronchial tree (Patrick and Stirling, 1977; Gore and Patrick, 1982; Watson and Brain, 1979; Radford and Martell, 1977; Svartengren et al., 1981). The mechanism(s) underlying this long-term retention is unknown, but may involve endocytosis by epithelial cells with subsequent translocation into deeper (submucosal) tissue, or merely passive movement into this tissue. In addition, uptake by the epithelium may depend upon the nature, or size, of the deposited particle (Watson and Brain, 1980). The retained particles may eventually be cleared to regional lymph nodes, but with a long half time that may be > 80 days (Patrick, 1989; Oghiso and Matsuoka, 1979).

There is some suggestion of a greater extent of long term retention in the bronchial tree. Stahlhofen et al. (1986), using a specialized inhalation procedure, noted that a significant fraction, up to 40%, of particles which were likely deposited in the conducting airways were not cleared up to six days post-deposition. They also noted that the size of the particles influenced this retention, with smaller ones being retained to a greater extent than were larger ones (Stahlhofen et al., 1987, 1990). Although the reason for this is not certain, the suggested presence of a surfactant film on the mucous lining of the airways (Gehr et al., 1990) may result in a reduced surface tension which, in turn, influences the displacement of particles into the gel layer and, subsequently, into the sol layer towards the epithelial cells. Particles that reach these cells may then be phagocytized, increasing retention time in the lungs. However, the issue of retention of large fractions of tracheobronchial deposit is not resolved.

Long-term TB retention patterns are not uniform. There is an enhancement at bifurcation regions (Cohen et al., 1988; Radford and Martell, 1977; Henshaw and Fews, 1984), the likely result of both greater deposition and less effective mucus clearance within these areas. Thus, doses calculated based upon uniform surface retention density may be misleading, especially if the material is, toxicologically, slow acting. Solubilized material may also undergo long-term retention in ciliated airways due to binding to cells or macromolecules.

Alveolar Region

Clearance kinetics in the A region are not definitively understood, although particles deposited there generally remain longer than do those deposited in airways cleared by mucociliary transport. There are limited data on rates in humans, while within any species rates vary widely due to different properties of the particles used in the various studies. Furthermore, some of these studies employed high concentrations of poorly soluble particles, which may have interfered with normal clearance mechanisms, producing rates different from those which would typically occur at lower exposure levels. Prolonged exposure to high particle concentrations is associated with what is termed particle "overload." This is discussed in greater detail in Section 10.4.2.7.

There are numerous pathways of A region clearance, and these may depend upon the nature of the particles being cleared. Thus, generalizations about clearance kinetics are difficult to make, especially since the manner in which particle characteristics affect clearance kinetics is not resolved. Nevertheless, A region clearance can be described as a multiphasic process, each phased considered to represent removal by a different mechanism or pathway, and often characterized by increased retention half-times with time post-exposure.

Clearance of inert, poorly soluble particles in healthy, nonsmoking humans has been generally observed to consist of two phases, with the first having a half-time measured in days, and the second in hundreds of days. Table 10-9 presents some observed times for the longer, second phase of clearance as reported in a number of studies. Differences in technique, chemistry, and solubility of the particles in Table 10-9 are largely responsbile for the variations. Although wide variations in retention reflect a dependence upon the nature of the deposited material (e.g., particle size) once dissolution is accounted for, mechanical removal to the gastrointestinal tract and/or lymphatic system appears to be independent of size, especially for particles $< 5\ \mu$m (Snipes et al., 1983). Although not evident from Table 10-9, there is considerable intersubject variability in the clearance rates of identical particles, which appears to increase with time post-exposure (Philipson et al., 1985; Bailey et al., 1985a). The large differences in clearance kinetics among different individuals suggest that equivalent chronic exposures to poorly soluble particles may result in large variations in respiratory tract burdens.

TABLE 10-9. LONG-TERM RETENTION OF POORLY SOLUBLE PARTICLES IN THE ALVEOLAR REGION OF NON-SMOKING HUMANS

Particle		Retention Half-Time[a]	
Material	Size (μm)	(days)	Reference
Polystyrene latex	5	150 to 300	Booker et al. (1967)
Polystyrene latex	5	144 to 340	Newton et al. (1978)
Polystyrene latex	0.5	33 to 602	Jammett et al. (1978)
Polystyrene latex	3.6	296	Bohning et al. (1982)
Teflon	4	100 to 2,500	Philipson et al. (1985)
Aluminosilicate	1.2	330	Bailey et al. (1982)
Aluminosilicate	3.9	420	Bailey et al. (1982)
Iron oxide (Fe_2O_3)	0.8	62	Morrow et al. (1967a,b)
Iron oxide (Fe_2O_3)	0.1	270	Waite and Ramsden (1971)
Iron oxide (Fe_3O_4)	2.8	70	Cohen et al. (1979)

[a]Represent the half-time for the slowest clearance phase observed.

While the kinetics of overall clearance from the A region have been assessed to some extent, much less is known concerning relative rates along specific pathways, and any available information is generally from studies with laboratory animals. The usual initial step in clearance, i.e., uptake of deposited particles by alveolar macrophages, is very rapid. Ingestion by macrophages generally occurs within 24 h of a single inhalation (Naumann and Schlesinger, 1986; Lehnert and Morrow, 1985). But the actual rate of subsequent macrophage clearance is not certain; perhaps 5% or less of their total number is translocated from the lungs each day in rodents (Lehnert and Morrow, 1985; Masse et al., 1974).

The rate and amount of particle uptake by macrophages is likely governed by particle size and surface properties (Tabata and Ikada, 1988), although these experiments were performed with peritoneal macrophages and not with alveolar macrophages. For example, the effect of particle size was examined by incubating mouse peritoneal macrophages with polymer microspheres (0.5 to 5 μm). Both the number of particles ingested per cell and the volume of these particles per cell reached a maximum for particle diameters of 1-2 μm, declining on either side of this range. In terms of particle surface, those with hydrophobic surfaces were ingested to a greater extent than were those with hydrophilic surfaces. Phagocytosis also increased as the

surface charge density of a particle increased, but for the same charge density there was no difference in uptake between positively or negatively charged particles.

The time for clearance of particle-laden alveolar macrophages via the mucociliary system depends upon the site of uptake relative to the distal terminus of the mucus blanket at the bronchiolar level. Furthermore, clearance pathways, and subsequent kinetics, may depend to some extent upon particle size. For example, some smaller ultrafine particles (perhaps < 0.02 μm) may be less effectively phagocytosed than are larger ones (Oberdörster, 1993). But once ingestion occurs, alveolar macrophage-mediated kinetics are independent of the particle involved, as long as solubility and cytotoxicity are low.

In terms of other clearance pathways, uningested particles may penetrate into the interstitium, largely by Type I cell endocytosis, within a few hours following deposition (Ferin and Feldstein, 1978; Sorokin and Brain, 1975; Brody et al., 1981). This transepithelial passage seems to increase as particle loading increases, especially to a level above the saturation point for increasing macrophage number (Adamson and Bowden, 1981; Ferin, 1977). It may also be particle size dependent, since insoluble ultrafine particles (<0.1 μm diameter) of low intrinsic toxicity show increased access to and greater lymphatic uptake than do larger ones of the same material (Oberdörster et al., 1992). However, ultrafine particles of different materials may not enter the interstitium to the same extent. Similarly, any depression of phagocytic activity or the deposition of large numbers of smaller ultrafine particles may increase the number of free particles in the alveoli, enhancing removal by other routes. In any case, free particles and alveolar macrophages may reach the lymph nodes, perhaps within a few days after deposition (Lehnert et al., 1988; Harmsen et al., 1985), although this route is not certain and may be species dependent.

The extent of lymphatic uptake of particles may depend upon the effectiveness of other clearance pathways. For example, lymphatic translocation probably increases when phagocytic activity of alveolar macrophages is decreased (Greenspan, et al., 1988). This may be a factor in lung overload, as discussed in Section 10.4.2.7. However, it seems that the deposited mass or number of particles must reach some threshold below which increases in loading do not affect translocation rate to the lymph nodes (Ferin and Feldstein, 1978; LaBelle and Brieger, 1961).

The rate of translocation to the lymphatic system may be somewhat particle size dependent. Although no human data are available, translocation of latex particles to the lymph nodes of rats was greater for 0.5 to 2 μm particles than for 5 and 9 μm particles (Takahashi et al., 1992), and smaller particles within the 3 to 15 μm size range were found to be translocated at faster rates than were larger sizes (Snipes and Clem, 1981). On the other hand, translocation to the lymph nodes was similar for both 0.4 μm barium sulfate or 0.02 μm gold colloid particles (Takahashi et al., 1987). It seems that particles $\leq$ 2 μm clear to the lymphatic system at a rate independent of size, and it is particles of this size, rather than those $\geq$ 5 μm, that would have significant deposition within the A region following inhalation.

In any case, and regardless of any particle size dependence, the normal rate of translocation to the lymphatic system is quite slow, on the order of 0.02-0.003%/day (Snipes, 1989), and elimination from the lymph nodes is even slower, with half-times estimated in tens of years (Roy, 1989).

Soluble particles depositing in the A region may be rapidly cleared via absorption through the epithelial surface into the blood, but there are few data on dissolution and transfer rates to blood in humans. Actual rates depend upon the size of the particle (i.e., solute size), with smaller ones clearing faster than larger ones. Chemistry also plays a role, since water soluble compounds generally clear at a slower rate than do lipid soluble materials.

Absorption may be considered as a two stage process, with the first stage dissociation of the deposited particles into material that can be absorbed into the circulation (dissolution) and the second stage the uptake of this material. Each of these stages may be time dependent. The rate of dissolution depends upon a number of factors, including particle surface area and chemical structure. Uptake into the circulation is generally considered as instantaneous, although a portion of the dissolved material may be absorbed more slowly due to binding to respiratory tract components. Accordingly, there is a very wide range for absorption rates depending upon the physicochemical properties of the material deposited. For example, a highly soluble particle may be absorbed at a rate faster than the particle transport rate and significant uptake may occur in the conducting airways. On the other

hand, a particle that is less soluble and remains in the lungs for years would have a much lower rate, perhaps <0.0001%/day.

10.4.2.5 Factors Modifying Clearance

A number of host and environmental factors may modify normal clearance patterns, affecting the dose delivered by exposure to inhaled particles. These include aging, gender, workload, disease and irritant inhalation. However, in many cases, the exact role of these factors is not resolved.

Age

The evidence for aging-related effects on mucociliary function in healthy individuals is equivocal, with studies showing either no changes or some slowing in mucous clearance function with age after maturity (Goodman et al., 1978; Yeates et al., 1981a; Puchelle et al., 1979). However, it is often difficult to determine whether any observed functional decrement was due to aging alone, or to long-term, low level ambient pollutant exposure (Wanner, 1977). In any case, the change in mucous velocity between approximately age 20 and 70 in humans is about a factor of two (Wolff, 1992) and would likely not significantly affect overall kinetics.

There are few data to allow assessment of aging-related changes in clearance from the A region. Although functional differences have been found between alveolar macrophages of mature and senescent mice (Esposito and Pennington, 1983), no age-related decline in macrophage function has been seen in humans (Gardner et al., 1981).

There are also insufficient data to assess changes in clearance in the growing lung. Nasal mucociliary clearance time in a group of children (average age = 7 yrs) was found to be ≈10 min (Passali and Bianchini Ciampoli, 1985); this is within the range for adults. There is one report of bronchial clearance in children (12 yrs old), but this was performed in patients hospitalized for renal disease (Huhnerbein et al., 1984).

Gender

No gender related differences were found in nasal mucociliary clearance rates in children (Passali and Bianchini Ciampoli, 1985) nor in tracheal transport rates in adults

(Yeates et al., 1975). Slower bronchial clearance has been noted in male compared to female adults, but this was attributed to differences in lung size (and resultant clearance pathway length) rather than to inherent gender related differences in transport velocities (Gerrard et al., 1986).

Physical Activity

The effect of increased physical activity upon mucociliary clearance is unresolved, with the available data indicating either no effect or an increased clearance rate with exercise (Wolff et al., 1977; Pavia, 1984). There are no data concerning changes in A region clearance with increased activity levels, but CO_2-stimulated hyperpnea (rapid, deep breathing) was found to have no effect on early alveolar clearance and redistribution of particles (Valberg et al., 1985). Breathing with an increased tidal volume was noted to increase the rate of particle clearance from the A region, and this was suggested to be due to distension related evacuation of surfactant into proximal airways, resulting in a facilitated movement of particle-laden macrophages or uningested particles due to the accelerated motion of the alveolar fluid film (John et al., 1994).

Respiratory Tract Disease

Various respiratory tract diseases are associated with clearance alterations. The examination of clearance in individuals with lung disease requires careful interpretation of results, since differences in deposition of tracer particles used to assess clearance function may occur between normal individuals and those with respiratory disease, and this would directly impact upon the measured clearance rates, especially in the tracheobronchial tree. In any case, nasal mucociliary clearance is prolonged in humans with chronic sinusitis, bronchiectasis, or rhinitis (Majima et al., 1983; Stanley et al., 1985), and in cystic fibrosis (Rutland and Cole, 1981). Bronchial mucus transport may be impaired in people with bronchial carcinoma (Matthys et al., 1983), chronic bronchitis (Vastag et al., 1986), asthma (Pavia et al., 1985), and in association with various acute infections (Lourenco et al., 1971; Camner et al., 1979; Puchelle et al., 1980). In certain of these cases, coughing may enhance mucus clearance, but it generally is effective only if excess secretions are present.

Normal mucociliary function is essential to respiratory tract health. Studies of individuals with a syndrome characterized by impaired clearance, i.e., primary ciliary dyskinesia (PCD),

may be used to assess the importance of mucociliary transport and the effect of its dysfunction upon respiratory disease, and to provide information on the role of clearance in maintaining the integrity of the lungs. The lack of mucociliary function in PCD is directly responsible for the early development of recurrent respiratory tract infections and, eventually, chronic bronchitis and bronchiectasis (Rossman et al., 1984; Wanner, 1980). It is, however, not certain whether partial impairment of the mucociliary system will increase the risk of lung disease.

Rates of A region particle clearance appear to be reduced in humans with chronic obstructive lung disease (Bohning et al., 1982) and in laboratory animals with viral infections (Creasia et al., 1973). The viability and functional activity of macrophages was found to be impaired in human asthmatics (Godard et al., 1982).

Studies with laboratory animals have also found disease related clearance changes. Hamsters with interstitial fibrosis showed an increased degree of alveolar clearance (Tryka et al., 1985). Rats with emphysema showed no clearance difference from control (Damon et al., 1983), although the co-presence of inflammation resulted in prolonged retention (Hahn and Hobbs, 1979). On the other hand, inflammation may enhance particle and macrophage penetration through the alveolar epithelium into the interstitium, by increasing the permeability of the epithelium and the lymphatic endothelium (Corry et al., 1984). Neutrophils, which are phagocytic cells present in alveoli during inflammation, may contribute to the clearance of particles via the mucociliary system (Bice et al., 1990).

Macrophages have specific functional properties, namely phagocytic activity and mobility, which allow them to adequately perform their role in clearance. Alveolar macrophages from calves with an induced interstitial inflammation (pneumonitis) were found to have enhanced phagocytic activity compared to normal animals (Slauson et al., 1989). On the other hand, depressed phagocytosis was found with virus-induced acute bronchiolitis and alveolitis (Slauson et al., 1987). How such alterations affect clearance from the A region is not certain, since the relationship between macrophage functional characteristics and overall clearance is not always straightforward. While changes in macrophage function do impact upon clearance, the manner by which they do so may not always be easily

predictable. In any case, the modification of functional properties of macrophages appear to be injury specific, in that they reflect the nature and anatomic pattern of disease.

Inhaled Irritants

Inhaled irritants have been shown to have an effect upon mucociliary clearance function in both humans and laboratory animals (Schlesinger, 1990; Wolff, 1986). Single exposures to a particular material may increase or decrease the overall rate of tracheobronchial clearance, often depending upon the exposure concentration (Schlesinger, 1986). Alterations in clearance rate following single exposures to moderate concentrations of irritants are generally transient, lasting < 24 h. However, repeated exposures may result in an increase in intra-individual variability of clearance rate and persistently retarded clearance. The effects of irritant exposure may be enhanced by exercise, or by coexposure to other materials.

Acute and chronic exposures to inhaled irritants may also alter A region clearance (Cohen et al., 1979; Ferin and Leach, 1977; Schlesinger et al., 1986; Phalen et al., 1994), which may be accelerated or depressed, depending upon the specific material and/or length of exposure. While the clearance of poorly soluble particles from conducting airways is due largely to only one mechanism, i.e., mucociliary transport, clearance from the respiratory region involves a complex of multiple pathways and processes. Because transit times along these different pathways vary widely, a toxicant-induced change in clearance rate could be due to a change in the time for removal along a particular pathway and/or to a change in the actual route taken. Thus, it is often quite difficult to delineate specific mechanisms of action for toxicants which alter overall clearance from respiratory airways. Alterations in alveolar macrophages likely underlay some of the observed changes, since numerous irritants have been shown to impair the numbers and functional properties of these cells (Gardner, 1984).

Since a great number of people are exposed to cigarette smoke, it is of interest to summarize effects of this irritant upon clearance processes. Smoke exposed animals and humans show increased number of macrophages recoverable by bronchopulmonary lavage (Brody and Davis, 1982; Warr and Martin, 1978; Matulionis, 1984; Zwicker et al., 1978). However, the rate of particle clearance from the A region of the lungs appears to be reduced in cigarette smokers (Bohning et al., 1982; Cohen et al., 1979).

While cigarette smoking has been shown to affect tracheobronchial mucociliary clearance function, the effects range from acceleration to slowing. Some of the apparent discrepancies in different studies is related to differences in the effects of short-term versus long-term effects of cigarette smoke. Long term smokers appear to have mucociliary clearance which is slower than that in nonsmokers (Lourenco et al., 1971; Albert et al., 1971) and which also show certain anomalies, such as periods of intermittent clearance stasis. On the other hand, the short term effects of cigarette smoke range from acceleration to retardation depending upon the number of cigarettes smoked (Albert et al., 1971; Lippmann et al., 1977; Albert et al., 1974).

10.4.2.6 Comparative Aspects of Clearance

As with deposition analyses, the inability to study the retention of certain materials in humans for direct risk assessment requires use of laboratory animals. Since dosimetry depends upon clearance rates and routes, adequate toxicologic assessment necessitates that clearance kinetics in these animals be related to those in humans. The basic mechanisms and overall patterns of clearance from the respiratory tract appear to be similar in humans and most other mammals. However, regional clearance rates can show substantial variation between species, even for similar particles deposited under comparable exposure conditions (Snipes, 1989).

Dissolution rates and rates of transfer of dissolved substances into the blood may or may not be species independent, depending upon certain chemical properties of the deposited material (Griffith et al., 1983; Bailey et al., 1985b; Roy, 1989). For example, lipophilic compounds of comparable molecular weight are cleared from the lungs of various species at the same rate (dependent solely upon solute molecular weight and the lipid/water partition coefficient), but hydrophilic compounds do show species differences.

On the other hand, there are distinct interspecies differences in rates of mechanical transport in the conducting and A airways. While mucous transport rates in the nasal passages seem to be similar in humans and the limited other species examined (Morgan et al., 1986; Whaley, 1987), tracheal mucous velocities vary among species as a function of body weight (Felicetti et al., 1981; Wolff, 1992).

In the A region, macrophage-mediated clearance of poorly soluble particles is species dependent, with small mammalian species generally exhibiting faster clearance than larger species, with the exception of the guinea pig which clears slower than laboratory rodents. This may result from interspecies differences in macrophage-mediated clearance of poorly soluble particles (Valberg and Blanchard, 1992; Bailey et al., 1985b), transport of particles from the A region to alveolar lymph nodes (Snipes et al., 1983; Mueller et al., 1990), phagocytic rates and chemotactic responses of alveolar macrophages (Warheit and Hartsky, 1994), or the prevalence of BALT (Murray and Driscoll, 1992). These likely result in species-dependent rate constants for these clearance pathways, and differences in regional (and perhaps total) clearance rates between some species are a reflection of these differences in mechanical processes. For example, the relative proportion of particles cleared from the A region in the short and longer term phases of clearance differs between laboratory rodents and larger mammals, with a greater percentage cleared in the faster first phase in laboratory rodents. The end result of interspecies differences in deposition and clearance is that the retention of deposited particles can differ between species, and this may result in differences in response to similar particulate exposure atmospheres.

10.4.2.7 Lung Overload

Some experimental studies using laboratory rodents employed high exposure concentrations of relatively nontoxic, poorly soluble particles, which interfered with normal clearance mechanisms, producing clearance rates different from those which would occur at lower exposure levels. Prolonged exposure to high particle concentrations is associated with what is termed particle "overload." This is defined as the overwhelming of macrophage-mediated clearance by the deposition of particles at a rate which exceeds the capacity of that clearance pathway. It is a nonspecific effect noted in experimental studies, generally in rats, using many different kinds of poorly soluble particles (including TiO_2, volcanic ash, diesel exhaust particles, carbon black, and fly ash) and results in A region clearance slowing or stasis, with an associated inflammation and aggregation of macrophages in the lungs and increased translocation of particles into the interstitium (Muhle et al., 1990; Lehnert, 1990; Morrow, 1994). While some overload induced effects are reversible, the extent of such reversibility decreases as the degree of overloading increases (Muhle et al., 1990). Once

some critical particle burden is reached, particles of all sizes (those studies ranged from ultrafine to 4 μm) show increased translocation into the interstitum (Oberdörster et al., 1992). This phenomenon has been suggested to be due to the inhibition of alveolar macrophage mobility.

While the exact amount of deposition needed to induce overload is uncertain, it has been hypothesized that it will begin, in the rat, when deposition approaches 1 mg particles/g lung tissue (Morrow, 1988). When the concentration reaches 10 mg particles/g lung tissue, macrophage-mediated clearance of particles would effectively cease. Overload may be related more to the volume of particles ingested than to the total mass (Morrow, 1988; Oberdörster et al., 1992b). Following overloading, the subsequent retardation of lung clearance, accumulation of particles, inflammation, and the interaction of inflammatory mediators with cell proliferative processes and DNA may lead to the development of tumors and fibrosis in rats (Mauderly, 1994).

Alternative hypotheses exist for the events that define the onset of lung overload. One hypothesis is that if repeated exposures to poorly soluble particles occurs, some critical lung burden may be reached. Until the critical lung burden is reached, clearance is normal; above the critical lung burden, clearance becomes progressively retarded and associated other changes occur. The other hypothesis is that overload is a function of the amount of poorly soluble particles which deposit daily, i.e., deposition rate (Muhle, 1988; Creutzenberg et al., 1989; Bellmann et al., 1990). Clearance retardation was suggested to occur at exposure levels of 3 mg/m^3 or higher. Thus, some critical deposition rate over a sufficient exposure duration would result in retardation of clearance (Yu et al., 1989).

The relevance of lung overload to humans, and even to species other than laboratory rats and mice, is not clear. While it likely to be of little relevance for most "real world" ambient exposures of humans, it is of concern in interpreting some long-term experimental exposure data. It may, however, be of some concern to humans occupationally exposed to some particle types (Mauderly, 1994), since overload may involve all insoluble materials and affect all species if the particles are deposited at a sufficient rate (Pritchard, 1989), (i.e., if the deposition rate exceeds the clearance rate). In addition, the relevance to humans is also clouded by the suggestion that macrophage-mediated clearance is normally slower and

perhaps less important in humans than in rats (Morrow, 1994), and that there will be significant differences in macrophage loading between the two species.

10.4.3 Acidic Aerosols

An Issue Paper on Acid Aerosols was published by the Environmental Protection Agency in 1989. Section 3 of that document was devoted to the deposition and fate of acid aerosols. Moreover, that Section provided an update of particle deposition data from both human and laboratory animal studies, described hygroscopic aerosol studies reported between 1977 and 1987, and presented a thorough discussion of the neutralization of acid aerosols by airway secretions and absorbed ammonia.

This section consists of two subsections: the first concerns the phenomenon of hygroscopicity; and the second presents current information on acidic aerosol neutralization.

10.4.3.1 Hygroscopicity of Acidic Aerosols

Hygroscopicity can be defined as the propensity of a material for taking up and retaining moisture under certain conditions of humidity and temperature. It is well known that action of ocean waves continuously disperses tons of hygroscopic saline particles into the atmosphere and these contribute to worldwide meteorologic phenomena. As industrialization has expanded, the evolution of gaseous pollutants, especially the oxides of sulfur and nitrogen, has caused a greatly increased atmospheric burden of aerosols mainly derived from gas-phase reactions. These aerosols are predominantly both acidic and hygroscopic, consisting of mixtures of partially neutralized nitric, sulfuric and hydrochloric acids: i.e., inorganic salts, such as nitrites, bisulfates, sulfates and chlorides. In addition, small amounts of organic acid salts, e.g., formate and acetate, are present as are a variety of trace elements, e.g., cadmium, carbon, vanadium, chromium and phosphorus, whose oxides and other chemical forms tend also to be acid forming (Aerosols, 1986).

Experimental studies on deposition of acid aerosols are limited. There have been two studies in laboratory animals using H_2SO_4 aerosols. Dahl and Griffith (1983) measured regional deposition of these aerosols in the size range from 0.4 to 1.2 μm MMAD generated at 20% and 80% relative humidities. Their data showed greater total and regional deposition of H_2SO_4 aerosols in rats compared to nonhygroscopic aerosols having the same MMAD's

(Figure 10-14). Deposition of H_2SO_4 aerosols generated at 20% RH was also higher than those generated at 80% RH, indicating that the increase in deposition was caused by the growth of the particles in the highly humid environment of the respiratory tract.

However, a similar study by Dahl et al. (1983) found that deposition of H_2SO_4 aerosols in beagle dogs at these two relative humidities was similar to that of nonhygroscopic aerosols having the same size although deposition at 20% RH was again higher than that at 80% RH. The inconsistent results were explained by Dahl et al. (1985) to be caused by the large intersubject variability of deposition in dogs.

Two reviews (Morrow, 1986; Hiller, 1991) have been published on hygroscopic aerosols which consider the implications of hygroscopic particle growth on deposition in the human respiratory tract. Much of the treatment of hygroscopic particle growth is based on theoretical models (e.g., Xu and Yu, 1985; Ferron et al., 1988; Martonen and Zhang, 1993). Suffice it to say, particulate sodium chloride has been commonly utilized in these models and to a lesser extent, sulfuric acid droplets, and ammonium sulfate and ammonium bisulfate particles. There are no major distinctions in the growth of these hygroscopic materials except that sulfuric acid does not manifest a deliquescent point (when the particle becomes an aqueous droplet). It can be seen in Figure 10-15 that the growth rate of hygroscopic particles is controlled by the relative humidity (RH): the closer to saturation (100% RH), the faster the growth rate.

In humans, deposition of acid aerosols in the respiratory tract has only been estimated by model studies. Martonen and Zhang (1993) estimated deposition of H_2SO_4 aerosols in the human lung for various ages and three different activity levels. The H_2SO_4 aerosol was considered to be in equilibrium with atmospheric conditions outside the lung prior to being inhaled. The results of their calculation for rest breathing without considering extrathoracic deposition are shown in Figure 10-16. Comparing to nonhygroscopic aerosols such as Fe_2SO_3, deposition of H_2SO_4 aerosols in different regions of the lung may be higher or lower depending upon the initial particle size. There is a critical initial size of H_2SO_4 in the 0.2 to 0.4 μm range. For larger particles the influence of hygroscopicity of H_2SO_4 aerosols is to increase total lung deposition, whereas for smaller particles the opposite occurs.

Hygroscopic particles or droplets of different initial size will experience different growth rates: the smallest particles being the fastest to reach an equilibrium size. For

Figure 7

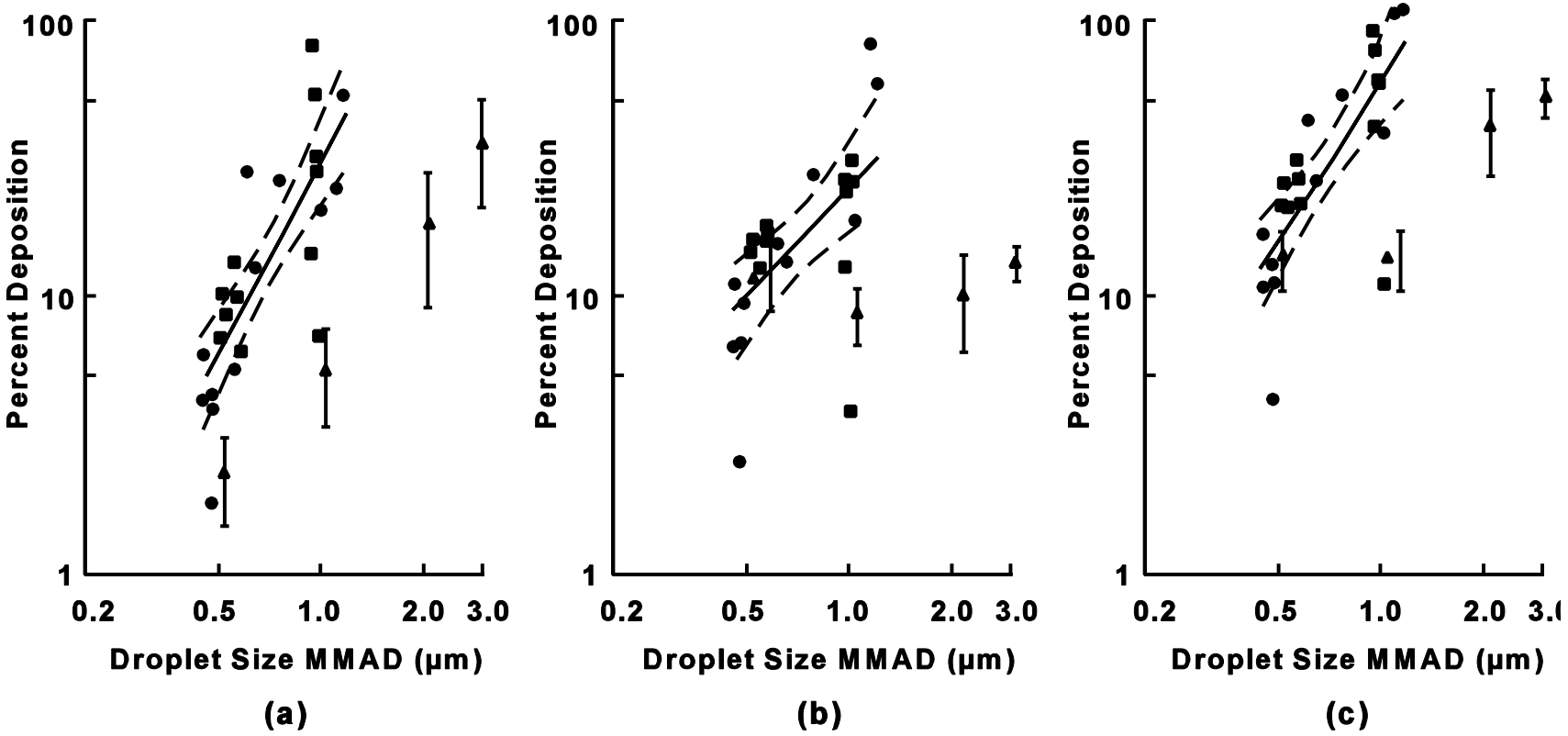

Figure 10-14. Regional deposition data in rats versus particle size for sulfuric acid mists and dry particles. Panel (a) = upper airway deposition; (b) = lower airway deposition; and (c) = total deposition. Circles are 20% relative humidity; squares are 80% relative humidity; triangles are dry nonhygroscopic particles. Solid curves represent the mean of the data for sulfuric acid mists. Error bars and broken curves represent 95% confidence limits.

Source: Dahl and Griffith (1983).

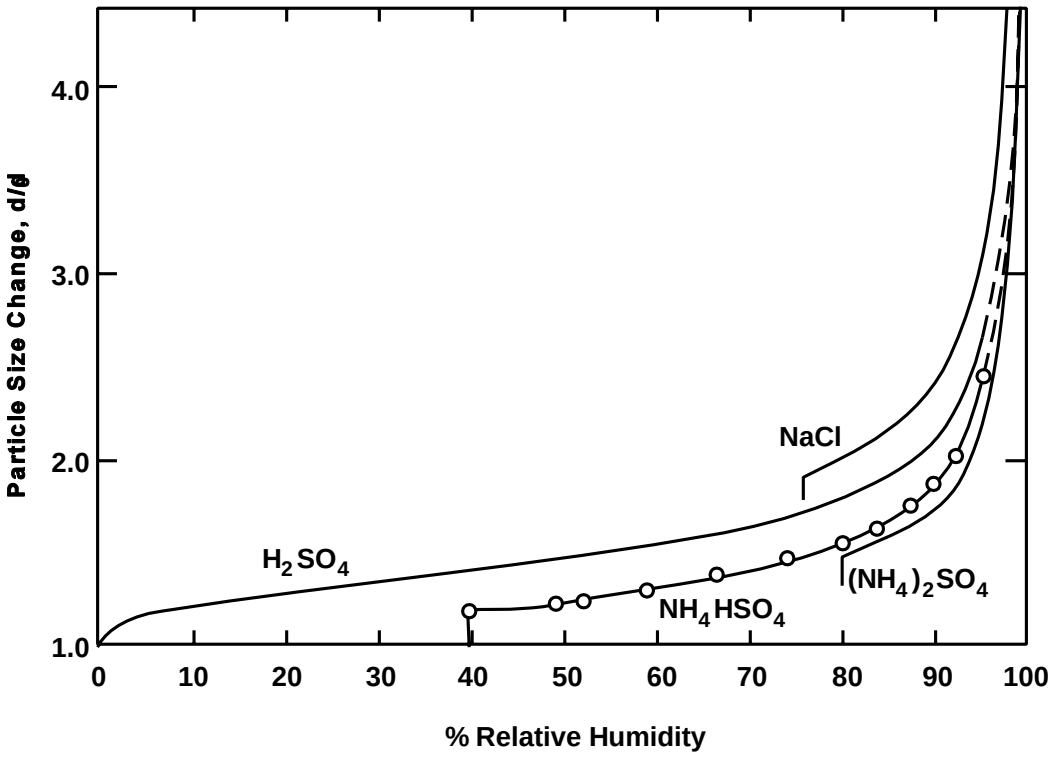

Figure 10-15. Theoretical growth curves for sodium chloride, sulfuric acid, ammonium bisulfate, and ammonium sulfate aerosols in terms of the initial (d_o) and final (d) size of the particle. Note that the H_2SO_4 curve, unlike those for the three salts, has no deliquescence point.

Source: Tang and Munkelwitz (1977).

example, a 0.5 μm diameter particle will require approximately 1 s, whereas a 2.0 μm particle will require close to 10 s. It is immediately evident that many inhaled hygroscopic particles will not reach their equilibrium size (maximum growth) during the duration of a single respiratory cycle (ca 4 s). Conversely, the growth of ultrafine particles does not resemble that for particles >0.1 μm and thereby represents a special case. Moreover, the hygroscopic growth characteristics of aqueous droplets, containing one or more solutes, depend not only on their initial size, but their initial composition. The study of Cocks and Fernando (1982), using the condensation model of Fukuta and Walter (1970), with ammonium sulfate droplets illustrate both of these last points (Figure 10-17).

The direct measurement of the RH of alveolar air and the temperature of air at the alveolar surface have been attempted, but because of technical limitations, the direct

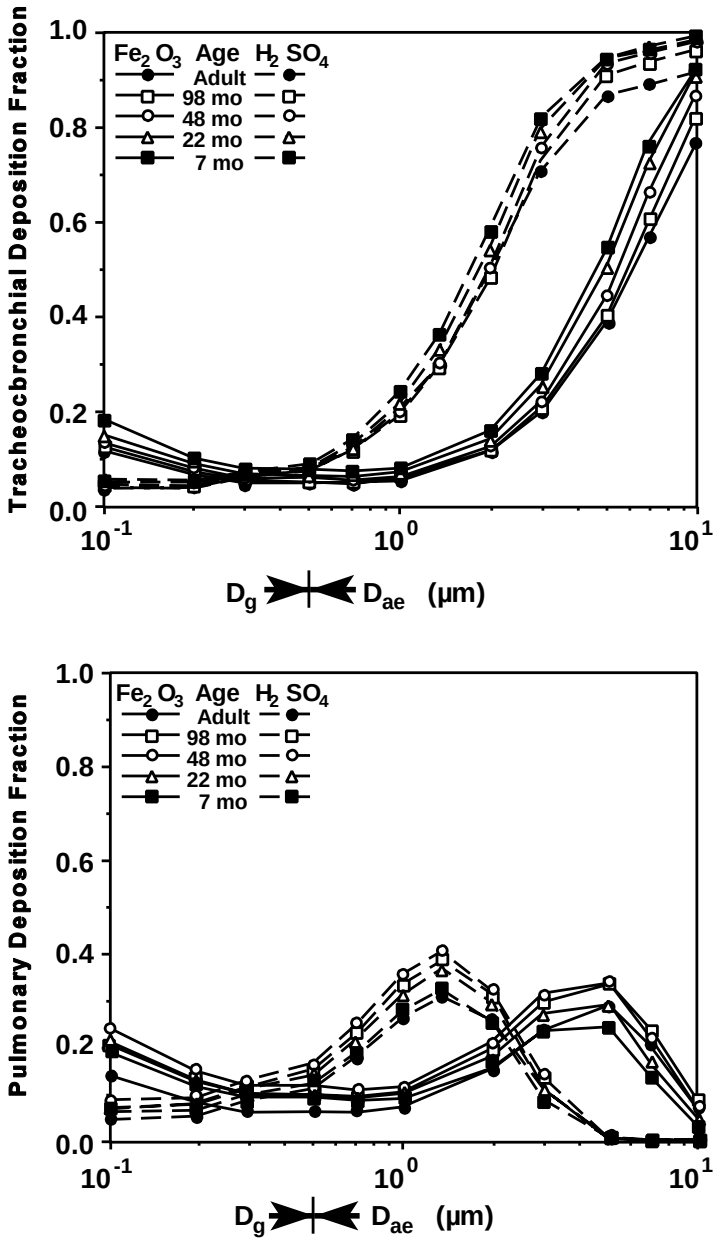

Figure 10-16. Regional deposition of hygroscopic sulfuric acid (H_2SO_4) and control iron oxide (FE_2O_3) particles at quiet breathing in the human lung as a function of subject age.

Source: Martonen and Zhang (1993).

experimental determinations of these and other values at different levels of the respiratory tract have only been considered reliable for conditions in the conducting airways (Morrow, 1986). Fortunately, indirect methods for these determinations have been

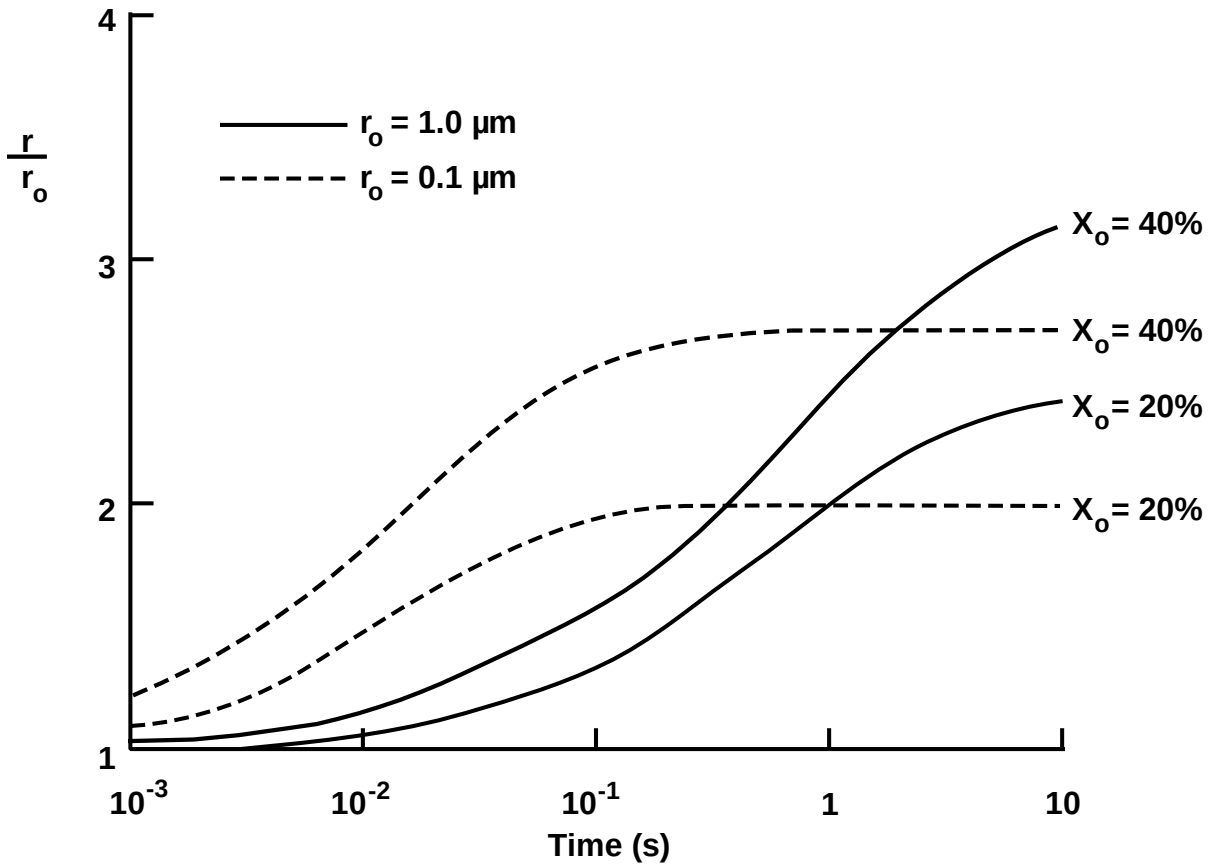

Figure 10-17. Distinctions in growth (r/r_o) of aqueous ammonium sulfate [$(NH_4)_2SO_4$] droplets of 0.1 and 1.0 μm initial size are depicted as a function of their initial solute concentrations (X_o).

Source: Cocks and Fernando (1982).

successful. For deep-lung temperature, Edwards et al. (1963) used solubility of a helium-argon mixture in arterial blood. By this approach they found the mean pulmonary capillary temperature in five normal subjects to be 37.52 °C. Because of individual variability, they also provided an equation for estimating the deep lung temperature in an individual from a measurement of rectal temperature.

Ferron and co-workers (1983, 1985) made the logical assumption that the RH of the alveolar air was determined by an equilibrium with the vapor pressure of blood serum at the capillary level. The osmolarity of serum at 37 °C (287 ± 4 mmol/kg) provided these investigators a sound basis for selecting 99.5% RH as the value to use in all of the modeling estimations. In Figure 10-18 (from Xu and Yu, 1985) the calculated equilibrium diameters

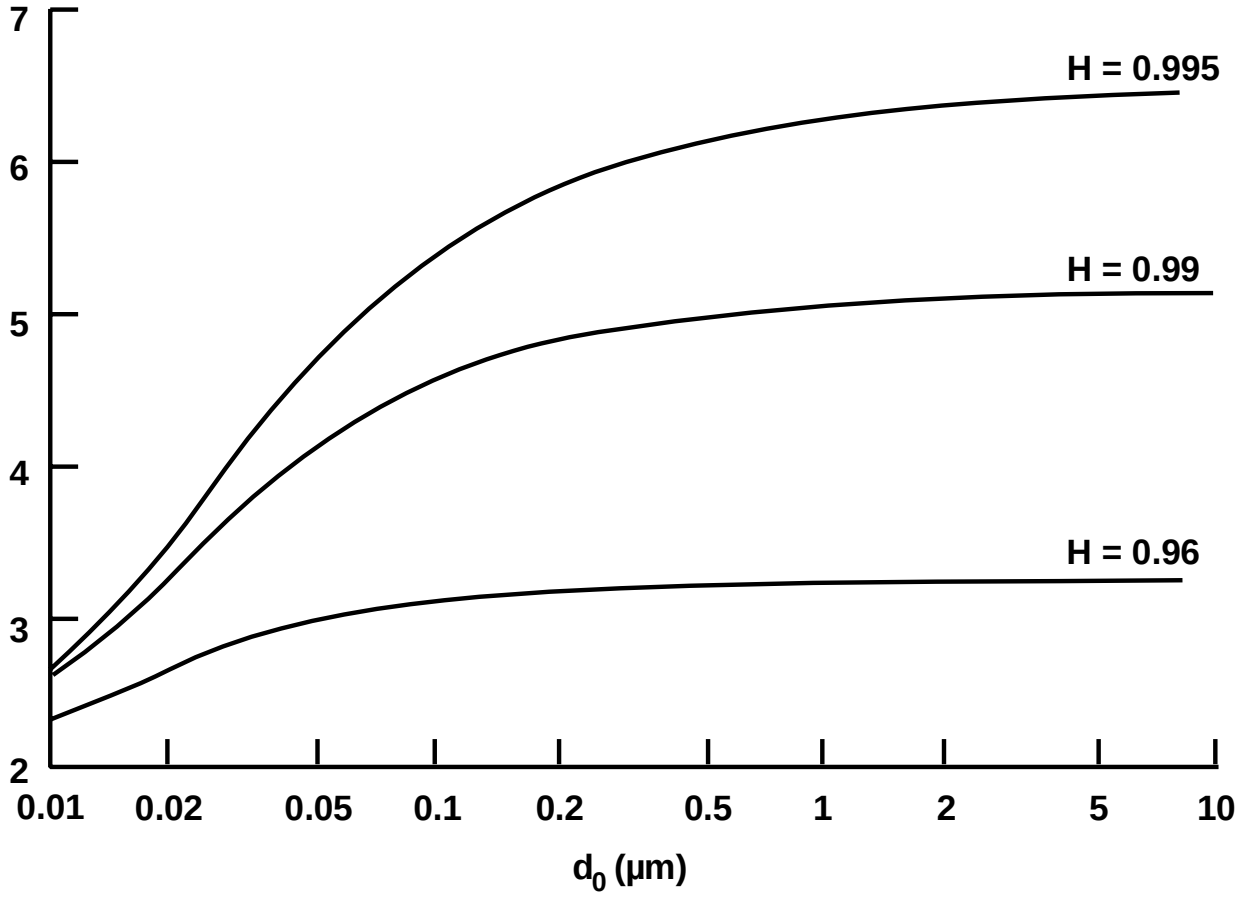

Figure 10-18. The initial diameter of dry sodium chloride particles (d_o) and equilibrium diameter achieved (d) are shown for three relative humidity assumptions.

Source: Xu and Yu (1985).

for sodium chloride particles on the basis of their initial size (d_o) is depicted. The equilibrium diameters (d_{oo}) that can be achieved theoretically for each particle size is shown as a function of three different RH values. For an RH of 99.5%, the growth of salt particles with an initial size greater than 0.5 µm, yields about a 6-fold increase in diameter.

Ferron et al. (1988) calculated the RH in the human airways by employing a transport theory for heat and water vapor using cylindrical coordinates. Several parameters of the theory were chosen to best fit the available experimental data. These authors also used the transport theory to model the growth and deposition of three salts, viz., NaCl, $CoCl_2 \cdot 6H_2O$,

and $ZnSO_4 \cdot 7H_2O$, which were selected because these differentially hydrated particles have large, moderate and small hygroscopic growth potentials, respectively. Figure 10-19 depicts the growth of these three salts when their initial dry particle size is 1.0 μm diameter, the average inspired airflow is 250 cc/s, and the inhalation is by mouth. In this depiction, the particle growth is expressed as the ratio of the achieved aerodynamic diameter to the initial aerodynamic size.

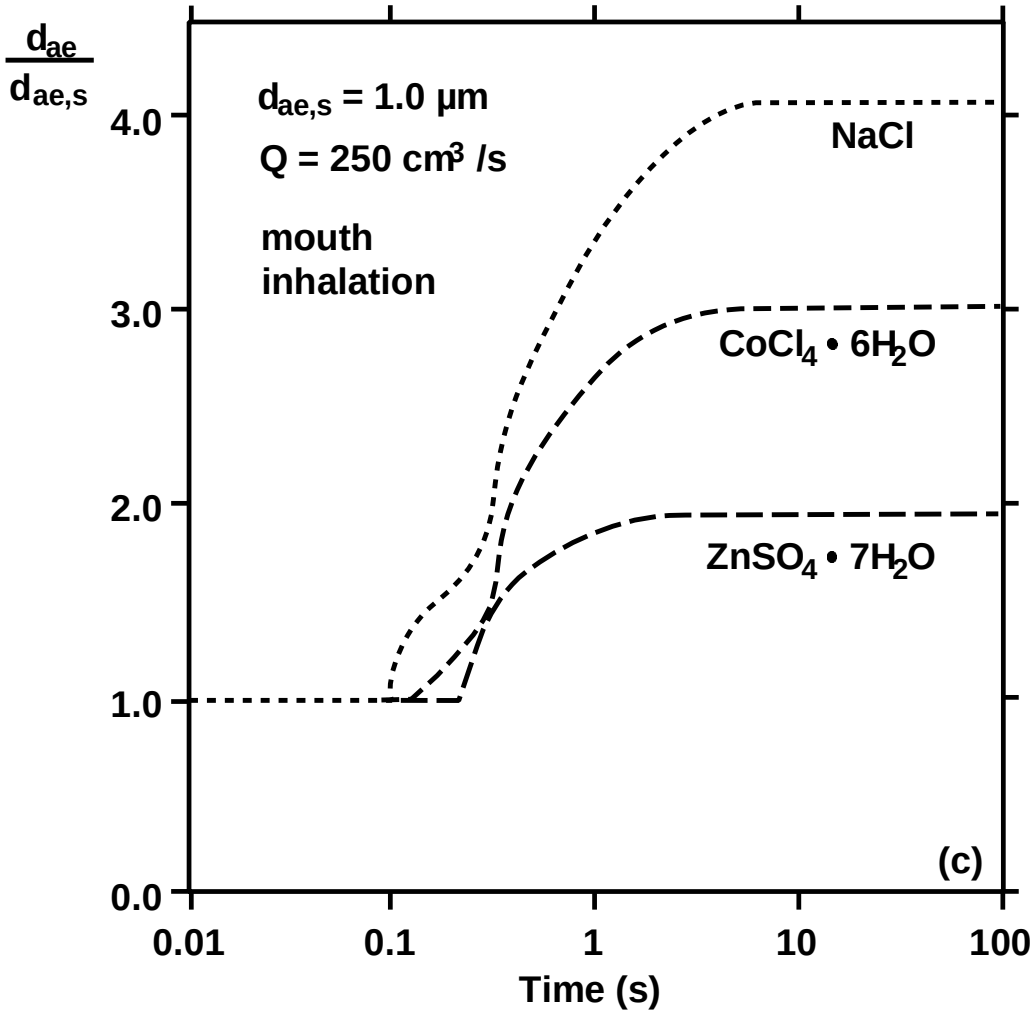

Figure 10-19. The initial dry diameter ($d_{ae,s}$) of three different salts is assumed to be 1.0 μm. Their subsequent growth to an equilibrium diameter at 99.5%RH is shown by the ratio ($d_{ae}/d_{ae,s}$). The highly hydrated salts of cobalt chloride and zinc sulfate exhibit a reduced growth potential compared to sodium chloride.

Source: Ferron et al. (1988).

A recent experimental study by Anselm et al. (1990) used an indirect method, similar to that employed earlier by Tu and Knudsen (1984), to validate the 99.5% RH assumption for alveolar air. In this instance, monodisperse NaCl particles between 0.2 and 0.5 μm were made by vibrating orifice generator and administered, by mouth, as boli during a constant inspiratory airflow. During expiration, the particles suspended in the same volume element were size classified. To determine equilibrium particle sizes, 600 mL of aerosol was inspired followed by 400 mL of clean air. Expiration was initiated after different periods of breath holding and the behavior of NaCl particles (loss and settling velocities) was compared to that of a stable (nonhygroscopic) aerosol. Through this approach, the investigators found that the diameters of the NaCl particles initially 0.2 μm and 0.25 μm, increased 5.55 and 5.79-fold, respectively. These values were found to be consistent with a 99.5% RH.

To make the transport theory model estimations more pragmatic, Ferron and coworkers (1992, 1993) made estimations for heterodisperse aerosols of salts with the range of growth potentials used in their 1988 study. Also, deposition estimates for H_2SO_4 aerosols, incorporating variabilities in age-related airway morphometry and in physical activity levels, have been reported by Martonen and Zhang (1993) using some innovative modeling assumptions.

In his excellent review of hygroscopic particle growth and deposition and their implications to human health, Hiller (1991) concluded that despite the importance of models, there remains insufficient experimental data on total and regional deposition of hygroscopic aerosols in humans to confirm these models adequately.

10.4.3.2 Neutralization and Buffering of Acidic Particles

The toxicity of acidic particles may be modulated following their inhalation. This may occur within the inhaled air, by neutralization reaction with endogenous respiratory tract ammonia, or following deposition, due to buffering within the fluid lining of the airways.

Reaction of Acidic Particles with Respiratory Tract Ammonia

Ammonia (NH_3) is present in the air within the respiratory tract. Measurements taken in exhaled air have found that the NH_3 concentration varies, depending upon the site of measurement, with levels obtained via oral breathing greater than those measured in the nose

or trachea (Larson et al., 1977; Vollmuth and Schlesinger, 1984). Because of these concentration differences between the oral and nasal passages, the route of acidic particle inhalation likely plays a significant role in determining the hydrogen ion (H^+) available for deposition in the lower respiratory tract. Thus, for the same mass concentration of acidic particles, inhalation via the mouth will result in more neutralization compared to inhalation via the nose, and less H^+ available for deposition in the lungs (Larson et al., 1982). The toxicity of acidic particles is likely due to the H^+, as discussed in Chapter 11.

The possibility that endogenous ammonia could chemically neutralize inhaled acidic particles to their ammonium salts prior to deposition on airway surfaces, thereby reducing toxicity, was originally proposed by Larson et al. (1977) in relation to acidic sulfate aerosols. Since, stoichiometrically, 1 μg of NH_3 can convert 5.8 μg of H_2SO_4 to ammonium bisulfate (NH_4HSO_4), or 2.9 μg of H_2SO_4 to ammonium sulfate [$(NH_4)_2SO_4$], they determined, based upon the range of NH_3 levels measured in the exhaled air of humans, that up to 1,500 $\mu g/m^3$ of inhaled H_2SO_4 could be converted to $(NH_4)_2SO_4$. For a given sulfate content in an exposure atmosphere, both ammonium bisulfate and ammonium sulfate are less potent irritants than is sulfuric acid.

Complete neutralization of inhaled sulfuric acid or ammonium bisulfate would produce ammonium sulfate. However, partial neutralization of sulfuric acid would reduce to varying extents the amount of H^+ available for deposition, thereby modulating toxicity. The extent of neutralization has been shown to play a role in measured toxicity from inhaled sulfuric acid. Utell et al. (1989) exposed asthmatic subjects to sulfuric acid under conditions of high or low levels of expired ammonia. The response to inhaled acid exposure was greater when exposure was conducted under conditions of low oral ammonia levels.

The extent of reaction of ammonia with acid sulfates depends upon a number of factors. These include residence time within the airway, which is a function of ventilation rate, and inhaled particle size. In terms of the latter, for a given amount of ammonia, the extent of neutralization is inversely proportional to particle size, at least within the diameter range of 0.1-10 μm (Larson et al., 1993). In addition, for any given ammonia concentration, the extent of neutralization of sulfuric acid increases as mass concentration of the acid aerosol decreases (Schlesinger and Chen, 1994).

Cocks and McElroy (1984) presented a model analysis for neutralization of sulfuric acid particles in human airways. Particle acidity was a function of both dilution by particle growth and neutralization by ammonia. As an example of their results, neutralization would be complete in 3 sec for H_2SO_4 (3M) having a particle size of 0.5 μm and a mass concentration of 100 $\mu g/m^3$, with the ammonia level at 500 $\mu g/m^3$. If the NH_3 level is reduced to 50 $\mu g/m^3$, neutralization would take longer.

Larson (1989) presented another model for neutralization of inhaled acidic sulfate aerosols in humans. It was concluded that significant deposition of acid in the lower respiratory tract would occur in the presence of typical respiratory tract NH_3 levels, for both oral or nasal inhalation of H_2SO_4 particles at 0.3μm. However, particles at 0.03μm should be completely neutralized in the upper respiratory tract. While this latter seems to contradict findings of significant biological responses in guinea pigs following exposure to ultrafine acid particles (Chapter 11), this could reflect differences in residence times and ammonia levels between different species. Furthermore, it is likely that under most circumstances, only partial neutralization of inhaled sulfuric acid occurs prior to deposition (Larson et al., 1977). In any case, these conclusions support toxicological findings of biological effects following inhalation of sulfuric acid concentrations that should, based solely upon stoichiometric considerations, be completely neutralized, and highlights the complexity of neutralization processes in the respiratory tract.

Larson et al. (1993) examined the role of ammonia and ventilation rate on response to inhaled (oral) sulfuric acid by estimating, using the model of Larson (1989), the acid concentrations to which the lungs would be exposed during oral inhalation. They concluded that combinations of high ammonia and low ventilation rate or low ammonia and high ventilation rate produce smaller or larger amounts of acid deposition, respectively, even if the acid concentration at the point of inhalation remained constant. The former condition resulted in greater neutralization than did the latter.

Buffering by Airway Surface Fluid (Mucus)

Mucus lining the conducting airways has the ability to buffer acid particles which deposit within it. The pH of mammalian tracheobronchial mucus has been reported to be within a range of about 6.5 to 8.2 (Boat et al., 1994; Gatto, 1981; Holma et al., 1977).

This variability may be due to differences in the methods used and species examined, as well as the likelihood that the acid-base equilibrium differs at different levels of the tracheobronchial tree, but may also reflect variations in secretion rate and the occurrence of inflammation. The influence on pH of various other endogenous factors, such as secretion of hydrogen or bicarbonate ions, and the role of specific mucus constituents, such as secreted acidic glycoproteins and basic macromolecules, have not been extensively examined.

The buffering capacity of human sputum, a mixture of saliva and mucus, was examined by Holma (1985), by titrating sputum equilibrated with 5% carbon dioxide at 37 °C and 100% relative humidity (RH) with sulfuric acid. While the buffering capacity was variable, depending upon the sputum sample examined, depression of pH from 7.25 to 6.5 required the addition of approximately 6 μmol of hydrogen ion (H^+) per milliliter of sputum. Assuming a tracheobronchial mucus volume of 2.1 mL, between 8 and 16 μmol of H^+, if evenly distributed through the airways, would be required to depress mucus pH from 7.4 to 6.5. Since 1 μg H^+ is obtained from 49 μg of sulfuric acid, between 390 and 780 μg of sulfuric acid would be required to cause this change in pH. With an inhalation exposure duration of 0.5 h, ventilation at 20 L/min and 50% deposition (in the total respiratory tract) of 100 $\mu g/m^3$ sulfuric acid (at 1M), 0.6 μmol of H^+ would be deposited in the lungs. However, the distribution of submicrometer acid particles in the respiratory tract is not uniform and, therefore, greater changes in pH may be anticipated on a regional basis in those areas having higher than average deposition. If, for example, 30 μg of acid deposited in 0.2 mL of mucus, a greater change in pH would likely occur.

The above example may apply to healthy individuals. However, the buffering capacity of mucus may be altered in individuals with compromised lungs. For example, sputum from asthmatics had a lower pH than that from healthy subjects, and a reduced buffering capacity (Holma, 1985). This group may, therefore, represent a portion of the population which is especially sensitive to inhaled acidic particles. The potential sensitivity of asthmatics to acid particles is discussed in greater detail in Chapter 11.

While biological responses following the inhalation of acidic aerosols are likely due to the H^+ component of these particles, it has been suggested that pH may not be the sole determinant of response to acid particles, but that response may actually depend upon total available hydrogen ion, or titratable acidity, depositing upon airway surfaces. Fine et al.

(1987) hypothesized that buffered acid aerosols (with a greater H^+ pool) would cause a greater biological response than would unbuffered acid aerosols having the same pH. Since airway surface fluids have a considerable capacity to buffer acid, it was suggested that the buffered acid would cause a more persistent decrease in airway surface fluid pH. Thus, it appears that the specific metric of acidity used, i.e., pH or titratable acid, would, therefore, be reflected in the relationship between amount of deposited acidity and resultant biological response.

10.5 DEPOSITION DATA AND MODELS

The background information in Sections 10.4 demonstrates that a knowledge of where particles of different sizes deposit in the respiratory tract and the amount of their deposition is necessary for understanding and interpreting the health effects associated with exposure to particles. As was seen, the respiratory tract can be divided into the ET, TB and A regions on the basis of structure, size and function. Particles deposited in the various regions have large differences in clearance pathways and, consequently, retention times. This section discusses the available data on particle deposition in humans and laboratory animals. Different approaches for modeling these data are also discussed. Theoretical models must assume average values and simplifying conditions of respiratory performance in order to make reasonable estimates. This latter approach was initiated by the meteorologist Findeisen (1935) over fifty years ago, when he developed a simplified anatomic model of the respiratory tract and assumed steady inspiratory and expiratory air flows in order to estimate the interactions between the anatomy of the respiratory tract and particle deposition based on physical laws. Despite much progress in respiratory modeling, there are not major distinctions in total particle deposition predictions among models and experimental verifications have been generally satisfactory.

10.5.1 Humans

The deposition of particles within the human respiratory tract have been assessed using a number of techniques (Valberg, 1985). Unfortunately, the use of different experimental methods and assumptions results in considerable variations in reported values. This section

discusses the available particle deposition data in humans for either the total respiratory tract or in terms of regional deposition.

10.5.1.1 Total Deposition

If the quantity of aerosol particles deposited in the entire respiratory tract is divided by that inhaled, the result is called total deposition fraction or total deposition. Thus, total deposition can be measured by comparing particle concentrations of the inhaled and exhaled, but the regional involvement cannot be distinguished. By the use of test aerosol particles with radiolabels, investigators have been able to separate deposition by region, beginning from the ET region with either nasal and nasopharyngeal deposition for nose breathing or oral and pharyngeal deposition for mouth breathing. The measurement of clearance of the radiolabeled particles from the thorax can be used to separate fast clearance, usually assumed to be an indicator of TB deposition, from the more slowly cleared A deposition (see below for more discussion).

Total human deposition data, as a function of particle size with nose and mouth breathing compiled by Schlesinger (1988) are depicted in Figure 10-20. These data were obtained by various investigators using different sizes of test spherical particles in healthy male adults under different ventilation conditions. Deposition with nose breathing is generally higher than that with mouth breathing because mouth breathing bypasses the filtration capabilities of the nasal passages. For large particles with aerodynamic diameters d_{ae} greater than 1 μm, deposition is governed by impaction and sedimentation and it increases with increasing d_{ae}. When $d_{ae} > 10$ μm, almost all inhaled particles are deposited. As the particle size decreases from 0.1 μm, diffusional deposition becomes dominant and total deposition depends more upon the physical diameter d of the particle. Decreasing particle diameter leads to an increase in total deposition in this particle size range. Total deposition shows a minimum for particle diameters in the range of 0.1 μm to 0.5 μm where neither sedimentation nor diffusion deposition are effective. The particle diameter at which the minimum deposition occurs is different for nose breathing and mouth breathing and it depends upon flow rate and airway dimensions. For all particle sizes, mixing of the tidal air and functional residual air can enhance particle deposition by providing a mechanism for keeping the inhaled particles in the lung for a longer time and

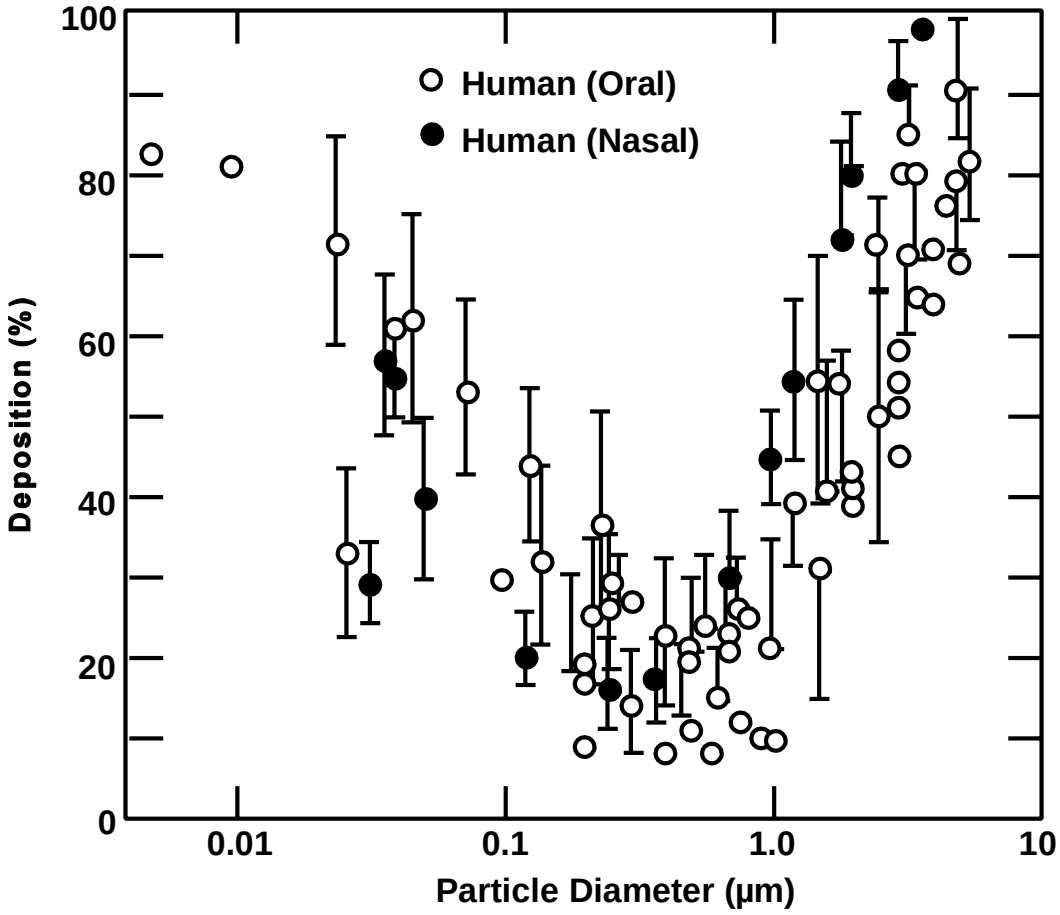

Figure 10-20. Total deposition data (percentage deposition of amount inhaled) in humans as a function of particle size. All values are means with standard deviations when available. Particle diameters are aerodynamic (MMAD) for those ≥ 0.5 μm.

Source: Schlesinger (1988).

thereby increasing the probability of the particles to deposit. This factor is more significant for particle sizes for which deposition is low. Good deposition experiments therefore should account for mixing into the residual volume by requiring subjects to fully exhale.

Although various studies in Figure 10-20 all appear to show the same trend, there is a significant amount of scatter in the data. Much of this scatter can be explained by the use of different test particles and methods in the experimental studies, as well as different breathing modes and ventilation conditions employed by the subjects. However, a good portion of the scatter is caused by the differences in airway morphology and breathing pattern among

subjects (Heyder et al., 1982, 1988; Yu et al., 1979; Yu and Diu, 1982a,b; Bennett and Smaldone, 1987; Bennett, 1988). In addressing the health-related issues of inhaled particles, this intersubject variability is an important factor which must be taken into consideration.

Indeed, for well controlled experiments and controlled breathing patterns (constant inspiratory flow in half a cycle and constant expiratory flow in another half cycle and no pause), total deposition data do not have the amount of scatter shown in Figure 10-20. Figure 10-21 shows the data by Heyder et al. (1986) and Schiller et al. (1986, 1988) reported by Stahlhofen et al. (1989) at controlled mouth breathing for particle size ranging from 0.005 μm to 15 μm and three different ventilation conditions. Total deposition was found higher for larger tidal volume while the minimum deposition occurred at about 0.4 μm for all three ventilation conditions.

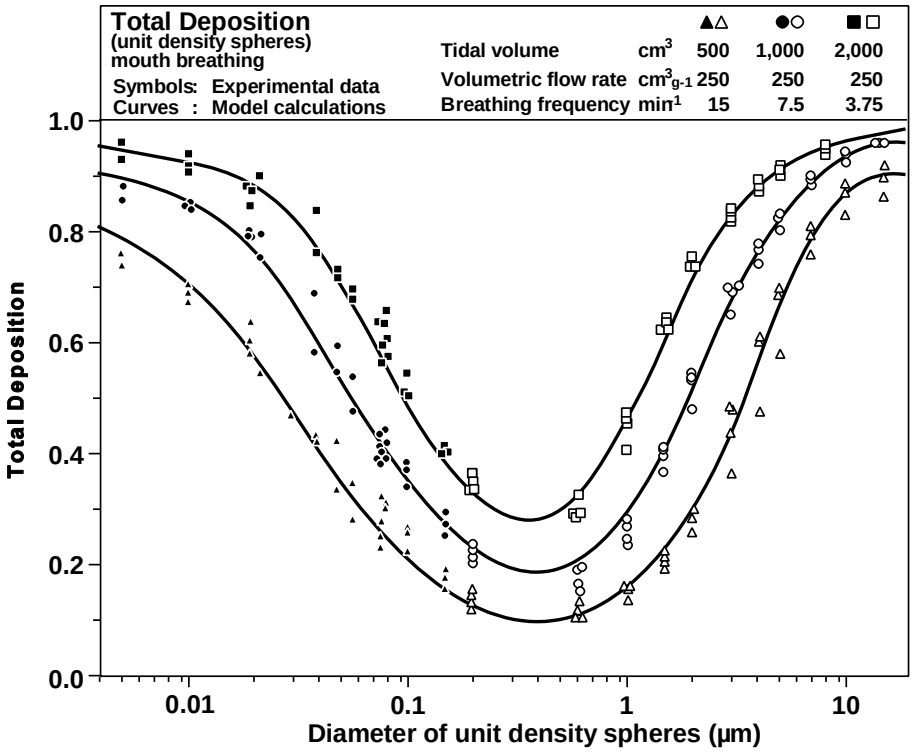

Figure 10-21. Total deposition as a function of the diameter of unit density spheres in humans for variable tidal volume and breathing frequency. Experimental data are by Heyder et al. (1986) and Schiller et al. (1988). The curves represent empirical fitting.

Source: Stahlhofen et al. (1988).